

N 71 - 18816

**NASA TECHNICAL
MEMORANDUM**

NASA TM X-52956

NASA TM X-52956

**A REVIEW OF NASA RESEARCH TO DETERMINE THE RESISTANCE OF
MATERIALS TO CAVITATION DAMAGE IN LIQUID METAL ENVIRONMENTS**

by Stanley G. Young and John C. Freche
Lewis Research Center
Cleveland, Ohio

TECHNICAL PAPER proposed for presentation at
International Conference on Corrosion Fatigue
University of Connecticut, Storrs, Connecticut, June 14-18, 1971

ABSTRACT

A long range program to investigate cavitation damage in liquid metal environments, conducted with a wide variety of materials at the NASA Lewis Research Center, is reviewed. A magnetostrictive vibratory apparatus was used to determine the cavitation damage resistance of iron-base, nickel-base, and cobalt-base alloys in liquid sodium and mercury. The combined effects of temperature and pressure of the cavitating liquid on the degree of material damage were determined. The interrelationships between material properties and cavitation damage were investigated. Extensive metallurgical studies were made to delineate the nature of material damage.

A REVIEW OF NASA RESEARCH TO DETERMINE THE RESISTANCE
OF MATERIALS TO CAVITATION DAMAGE IN
LIQUID METAL ENVIRONMENTS

by Stanley G. Young and John C. Freche

Lewis Research Center
National Aeronautics and Space Administration
Cleveland, Ohio

SUMMARY

This paper is a review of a long range program conducted to study cavitation damage in mercury and liquid sodium of materials under consideration for components of liquid metal power conversion systems. The effects of pressure and temperature of the cavitating liquid on cavitation damage were determined. Extensive metallurgical studies were made to delineate the nature of material damage.

A magnetostrictive vibratory apparatus was used to determine the cavitation damage resistance of iron-base, nickel-base, and cobalt-base alloys in liquid sodium at temperatures of 204^o, 427^o, and 649^o C and in mercury at 149^o C. The materials investigated in both sodium and mercury ranked in the same order of resistance to cavitation damage, but the degree of damage to all materials was consistently greater in mercury. The most resistant material investigated was the cobalt-base alloy, Stellite 6B.

Increasing the pressure from 1×10^5 to 4×10^5 N/m² (1 to 4 atmospheres) of the sodium significantly increased cavitation damage to the materials considered at all temperatures. This result indicated that in fluid systems where cavitation occurs in high pressure regions, damage to components may be much greater than would be expected from accelerated cavitation tests conducted at atmospheric pressure in the laboratory.

Metallographic studies indicated that the predominant feature of cavitation damage was undercutting; also, some subsurface deformation and transgranular cracking was noted. A striking similarity in damage characteristics was observed for materials tested in liquid sodium and distilled water. This lends credence to the view that cavitation damage resulting from ultrasonic vibratory testing is primarily mechanical in nature rather than chemical.

INTRODUCTION

Cavitation damage to materials occurs in many engineering applications where bubbles formed by transient low pressures in moving liquids, collapse rapidly on or near solid surfaces. In advanced space power conversion systems that use liquid metals for the heat-transfer medium cavitation damage can occur in components such as pump impellers or in stationary sections of these systems where local pressure fluctuations occur in the fluid. Damage is manifested in the form of pitting and surface erosion and has been observed in such components after relatively short test

times in liquid metal loops (refs. 1 to 3). Damage has also been observed in the turbine component of liquid-metal systems when the vapor quality is less than 100 percent (ref. 4). The cavitation damage problem is of particular importance in space power systems because these must function continuously for 10 000 hours or longer. A comprehensive series of investigations was therefore undertaken at the NASA Lewis Research Center to determine the resistance to cavitation damage in liquid metals of a wide variety of materials that might be used in various components of such systems, and to achieve a better understanding of the cavitation phenomenon in liquid metal environments and how it causes material damage. The results of those investigations are reviewed in this paper.

Extensive research has been conducted to study the mechanism of cavitation, cavitation damage, and impingement (refs. 6 to 17). A particularly comprehensive review is given in Ref. 8. In moving fluids where local pressures fall below the vapor pressure of the fluid, cavities form. When these cavities are swept into regions of higher pressure, they collapse with high velocity. If the collapse is on or near a metal surface the liquid can impinge on the surface causing localized high stresses in the metal and severe damage can result. Although much of this damage is of a mechanical nature, corrosion can also be a contributing factor (refs. 10 and 15). Attempts have been made to utilize conventional engineering properties such as hardness, tensile and yield strengths,

fatigue limit; and even corrosion resistance as a means of ranking materials with respect to cavitation damage. None of these properties individually provides a satisfactory criterion for rating materials; however, there is some evidence (ref. 18) that strain energy may correlate with the intensity of cavitation damage for a number of materials.

In order to study a great number of materials in relatively short times, various accelerated test methods for producing cavitation damage have been devised. These include the rotating-disk method (ref. 13), venturi systems (ref. 19), and ultrasonic vibration systems (ref. 15). All these methods have been adapted for use in liquid-metal environments (refs. 14, 20, and 21).

Of these various methods (refs. 14, 20, and 21), the ultrasonic vibration technique has become the most widely accepted. Recently, the ASTM G-2 Committee on Cavitation by Erosion or Impingement coordinated a carefully controlled series of round-robin tests (ref. 22) in which several different types of ultrasonic vibration devices were used and in which eleven laboratories, including the Lewis Research Center, participated (ref. 23). Despite differences in the individual test apparatuses, good agreement was noted in the relative ranking of materials for cavitation damage resistance.

A magnetostrictive vibratory apparatus was used in the NASA investigation and a wide variety of iron-base, nickel-base, and cobalt-base

alloys was studied. The bulk of the work was done in liquid sodium at 427° C and in mercury at 149° C under atmospheric pressure. Three materials with widely different mechanical properties were also investigated in liquid sodium while pressures ranging from 1×10^5 to 4×10^5 N/m² (1 to 4 atmospheres) were maintained on the cavitating fluid. Both fluid pressure and temperature were varied in the case of one material that was studied. This was done to assess the effect of temperature and pressure on cavitation damage. Materials were ranked according to their resistance to cavitation damage by material volume loss, volume loss rate, and surface roughness. Metallographic studies were made to determine the nature of the early stages of cavitation damage and to characterize long-time damage effects. Attempts were also made to correlate accelerated cavitation test data with cavitation damage sustained in actual pump operation in liquid-metal loops.

MATERIALS, APPARATUS, AND PROCEDURE

Materials

The materials tested for resistance to cavitation damage were the iron-base alloys Sicromo 9M, A-286, and AISI types 316 and 318 stainless steels; nickel-base alloys, Inconel 600, Hastelloy X, and René 41; and cobalt-base alloys, L-605 and Stellite 6B. The nominal chemical composition of each alloy is listed in Table 1. The heat treatments employed as well as the densities of these alloys are listed in Table 2.

Because of the wide differences in resistance to cavitation damage they exhibited in sodium at atmospheric pressure, AISI 316 stainless steel, and the cobalt-base alloys, L-605 (HS-25) and Stellite 6B were chosen to determine the effect of pressure of the cavitating fluid on cavitation damage. Tests in which both temperature and pressure of the cavitating fluid (sodium) were varied were conducted with L-605.

Reactor grade sodium (99.95 percent purity) and triple-distilled mercury were used as the test fluids. Chemical analyses indicated an initial oxygen level of 10 ppm for the sodium. Purity of the sodium was maintained by the addition of a titanium-sponge hot trap to the liquid metal bath and periodically heating to 649^o C for 3 to 4 hours. The mercury had less than 0.2 ppm total initial impurity content and was changed periodically to maintain purity.

Accelerated Cavitation Damage Test Facility

The apparatus used is shown schematically in Fig. 1. A more complete description of the facility and test procedure is given in Ref. 24. This figure illustrates the dry box arrangement, magnetostrictive transducer assembly, and separately sealed liquid metal test chamber with associated argon line, vapor trap, and pressure gage. The dry box and test chamber were designed to be evacuated to a pressure of approximately 0.13 N/m^2 (10^{-3} torr) and backfilled with high purity argon prior to testing.

The transducer assembly is shown in the photograph of Fig. 2. The specimen was attached to the end of a resonant system consisting of the transducer, exponential horn, and an extension rod specimen holder. The horn served as a displacement amplifier and provided a convenient attachment for a nodal flange vapor seal. The amplitude and frequency of vibration were detected by a magnetic pickup and read on an oscilloscope. An automatic feedback system maintained a constant amplitude of vibration irrespective of variations in resonant frequency induced by temperature changes. The output of the magnetic pickup was calibrated against measurements of amplitude made optically with a 200-power microscope.

After the liquid bath was brought to temperature, the transducer assembly was lowered into position. A sleeve attached to the nodal flange on the amplifying horn sealed the liquid-metal test chamber from the dry box, and the test chamber pressure was regulated through a separate argon line. Pressures were measured with a precision gage having an accuracy of 0.25 percent and temperature was controlled from a thermocouple directly immersed in the bath.

Test Conditions

The sodium tests were run at 204^o, 427^o, and 649^o C. The pressures maintained on the cavitating fluid ranged from 1×10⁵ to 4×10⁵ N/m². The fluid temperature was controlled to ±6^o C and pressure variations were

less than $1.7 \times 10^3 \text{ N/m}^2$. The mercury tests were all run at $149^\circ \text{ C} \pm 16^\circ \text{ C}$ under atmospheric pressure. The frequency of vibration of the test specimens was nominally 25 000 Hz, and the peak-to-peak displacement amplitude was $4.45 \times 10^{-2} \text{ mm} \pm 1.2 \times 10^{-3} \text{ mm}$. The specimen surface was immersed to a depth of approximately 3.3 mm.

Test Procedure

The type of specimen used is shown in Fig. 3. The test surface of each specimen was metallographically polished before testing to allow meaningful metallographic examination of the specimen surface during the early stages of damage.

Prior to the test, the specimens were cleaned, weighed, and photographed. After each time increment of cavitation exposure, the specimens were removed from the apparatus, cleaned, weighed, and rephotographed. Weight loss measurements were divided by density to obtain volume loss.

Test duration was dependent on the volume-loss rate for each material at each condition. In most cases, the testing of a specimen was continued for a sufficient time to achieve a relatively constant volume loss rate.

Surface roughness traces were obtained from the uniformly damaged portions of some of the specimens at various time increments. These were obtained with a linear profiler having a diamond stylus with a 0.013 mm radius and a cone angle of 51.5° . Usually a single trace approximately

0.675 cm in length was taken. When several different traces were taken on the same specimen, the arithmetic average surface roughness values were in agreement within approximately 12 percent.

After testing, some specimens were sectioned axially and examined metallographically to determine the depth of cavitation attack and to study the nature of cavitation damage to these materials.

RESULTS AND DISCUSSION

Validity of the Ultrasonic Vibratory Test Method

Of the many methods used to evaluate materials for resistance to cavitation damage, the vibratory method has become the most universally accepted. Various types of vibratory test facilities designed to impose accelerated cavitation damage on materials by subjecting them to high frequency vibration in a fluid have been used in laboratories for many years (refs. 25 and 26). Because of differences in test conditions such as amplitude and frequency of vibration, temperature, etc. employed by investigators using vibratory tests, it has been difficult to compare the results from one laboratory with those of another.

During 1967, the ASTM Committee G-2, on Erosion by Cavitation or Impingement, initiated a round-robin test program in which comparative tests were made with vibratory test facilities available at different laboratories. NASA participated in this program in which, as far as possible, test conditions were standardized. Thus, specimens from the

same original batch of material were tested in each laboratory. The three materials chosen for the program were type 316 stainless steel, nickel 270, and 6061-T6 aluminum. The major requirements of the G-2 committee were that the specimens be tested in distilled water at 23.9° C and atmospheric pressure. The specimen surface finish was 0.8 microns rms or better. Tests were carried out to at least 0.076 mm mean depth of penetration based upon total specimen surface area. Where possible a total displacement amplitude of 0.051 mm was used.

Despite differences in the individual test apparatuses, by keeping close control on test conditions, good agreement was obtained in the relative ranking of materials for cavitation damage resistance by the various participating laboratories. The ranking was, in order of decreasing resistance to cavitation damage, stainless steel, nickel, and aluminum. The results of this investigation are summarized in Ref. 22.

Ranking of Materials

When evaluating materials for their resistance to cavitation damage, it is necessary to rank them according to some parameter such as weight or volume loss. Because of the wide variety of materials, and the different cavitation damage rates encountered at various times during testing with different materials, an all-inclusive method of ranking materials for their resistance to cavitation damage has not been established. In this paper, three different methods for ranking materials are presented

in order to give a more complete overall picture of the relative resistance to cavitation damage of the materials tested. These methods are (1) total volume loss, (2) volume loss rate, both average (ref. 27) and "steady state" volume loss rate (refs. 28 and 29), and (3) surface roughness measurements.

Volume loss. - Cavitation damage is expressed as total volume loss for nine materials tested in sodium and five materials tested in mercury under 1×10^5 N/m² pressure in Figs. 4(a) and (b), respectively (ref. 24). The materials tested in sodium were ranked in order of increasing damage as follows: Stellite 6B, René 41, L-605, Hastelloy X, A-286, Inconel 600, AISI type 318 stainless steel, AISI type 316 stainless steel, and annealed Sicromo 9M. A wide range of damage was observed for the various materials. For example, after 4 hours the most resistant material, Stellite 6B, exhibited approximately 15 percent of the damage sustained by L-605, another of the more resistant alloys, but only approximately 2 percent of the damage sustained by annealed Sicromo 9M, the most heavily damaged material.

The materials tested in mercury were ranked in order of increasing damage as follows: Stellite 6B, hardened Sicromo 9M, L-605, Hastelloy X, and annealed Sicromo 9M. Again, a wide range in the degree of damage was observed. For example, after 4 hours, the most resistant material, Stellite 6B, showed approximately 16 percent of the

damage sustained by L-605; and after 1 hour, approximately 2 percent that of annealed Sicromo 9M.

Annealed Sicromo 9M with an original hardness of Rockwell B-80 was heat treated to a hardness of Rockwell C-40. At 1 hour the hardened alloy showed only about 6 percent of the damage sustained by this alloy in the annealed condition. Increasing the hardness substantially increased resistance to cavitation damage.

Volume loss rate. - Curves of volume loss rate are shown in Figs. 5(a) and (b). These curves represent the first derivative of the volume loss from Figs. 4(a) and (b) plotted as a function of time. Smooth curves were drawn through the volume loss data for AISI type 316 stainless steel, Inconel 600, A-286, Hastelloy X, and Stellite 6B, in order to reduce the effect of scatter. The first derivatives of these curves were used to obtain the volume loss rate curves shown in Figs. 5(a) and (b). The same procedure was employed for the remaining materials in Figs. 4(a) and (b), but because the volume loss data points for the latter materials were more widely spaced in time and because the exact shape of these curves is uncertain, portions of the rate curves (figs. 5(a) and (b)) for these materials are dashed.

A previous investigation (ref. 30) showed that materials tested for long times in water first reached a relatively steady-state damage condition but showed a decreasing damage rate after very long test times. In

order to limit test times to a reasonable length and at the same time to achieve a meaningful ranking of materials with respect to their resistance to cavitation damage, a steady-state damage rate was used as a criterion. The steady-state region is defined in the present investigation as that portion of the volume loss rate curves where the rate does not change over an extended period of time, and accurate, repeatable values for damage rate can be determined readily. In most cases, this occurred after peak damage rate was observed.

When the materials were compared on the basis of their steady-state damage rate, they were found to be ranked in the same order with respect to their resistance to cavitation damage as when compared on the basis of total volume loss.

Surface roughness measurements. - Because cavitation damage is usually measured quantitatively in terms of weight or volume loss, damage to system components, such as tubing or impellers, is sometimes difficult to measure accurately because of limited accessibility. If a correlation should exist between volume loss and surface roughness measurements, the latter might possibly be used to measure quantitatively the cavitation damage to these components. Cavitation damage was therefore measured in terms of surface roughness for all the materials tested in mercury and five of the materials tested in sodium.

A comparison of the arithmetic average surface roughness with volume

loss as a function of test time in sodium and in mercury is shown in Figs. 6(a) and (b), respectively. These materials ranked in the same order on the basis of both surface roughness and volume loss. Surface roughness measurements are extremely sensitive, and a clear distinction among the materials as to relative cavitation damage resistance can be made by this method during the early stages of damage, even though very little volume loss has occurred.

Comparison of Cavitation Damage Resistance of Materials in Sodium and Mercury

Although the materials tested in both sodium and mercury ranked in the same order of resistance to cavitation damage (fig. 4) the severity of cavitation damage experienced by all materials in mercury at 149°C was two to seven times greater on the basis of total volume loss than that experienced by the same material in sodium at 427°C .

Volume loss rate values (fig. 5(b)) were also much higher in mercury than in sodium; however, steady-state rates for mercury cavitation damage were not as clearly defined as in the case for sodium. The surface roughness values for cavitation damage in mercury (fig. 6(b)) were also several times greater than those measured after testing in sodium. These results suggest that the nature of attack by mercury is quite different from that by sodium, and this will be discussed in the section of this paper dealing with the metallurgical aspects.

- Relation Between Accelerated Cavitation Damage Test Results
and Cavitation Damage Observed in Pump Impellers

A qualitative comparison was made between the damage experienced by three materials (René 41 and AISI types 316 and 318 stainless steel) tested in the accelerated cavitation damage facility and that experienced by the same materials when used as pump impeller vanes in sodium loop tests conducted at the Lewis Research Center (ref. 31). Visual observations indicated that the materials ranked in the same order with respect to resistance to cavitation damage after accelerated tests as after actual pump loop operation under cavitating conditions.

Macrographs of the damaged surfaces of impeller blades that were operated for 250 hours under cavitating conditions at temperatures up to 816°C are shown in Fig. 7. The René 41 impeller blade showed virtually no cavitation damage; whereas, the AISI types 318 and 316 stainless steel blades had regions of marked damage. The degree of damage for the two stainless-steel blades was not appreciably different. When the materials are considered on the basis of volume loss in the accelerated tests (fig. 4(a)), René 41 shows considerably less damage than either of these steels. Both steels, however, ranked very closely with respect to volume loss. It is significant that a qualitative agreement between the results of accelerated cavitation tests and full-scale impeller operation was obtained. Surface traces were taken of the damaged areas of the impeller blades

in an attempt to determine a quantitative measure of the cavitation damage. However, the extent of general corrosion of the blade surfaces masked the degree of localized cavitation damage. From this it is evident that measurements of surface roughness should have been made earlier in these tests in order to adequately use this means of measuring cavitation damage. In any event, these results suggest that the vibratory type of accelerated cavitation test can provide a useful means of selecting materials suitable for long time operation under cavitating conditions.

Effect of Pressure of Cavitating Liquid on Cavitation Damage

In power conversion systems, fluid pressure can vary, depending on the operating conditions, from near the fluid vapor pressures at the pump inlet to many atmospheres of pressure at the pump outlet. Similarly in submersible vehicles for marine applications, ambient fluid pressures can increase significantly with depth. Therefore, it is important to establish the effect of pressure on cavitation damage to materials in order to achieve a better understanding of the cavitation phenomenon which is encountered in many different engineering applications.

Three materials - AISI type 316 stainless steel and the cobalt-base alloys L-605 (HS-25) and Stellite 6B were chosen to study the effect of pressure of the cavitating fluid on cavitation damage. These materials had previously shown wide differences in their resistance to cavitation damage at atmospheric pressure. AISI type 316 stainless steel showed

low resistance to cavitation damage. L-605 showed intermediate resistance and Stellite 6B was the most damage-resistant alloy evaluated.

The effect of pressure on cavitation damage to L-605 at 1×10^5 , 2×10^5 , 3×10^5 , and 4×10^5 N/m² is shown in terms of volume loss and volume loss rate in Figs. 8(a) and (b), respectively. From this figure, it is evident that cavitation at higher pressures resulted in (1) higher cumulative volume loss, (2) a higher volume loss rate peak, and (3) a higher level of steady-state volume loss rate. It is interesting that the shape of the rate curve varies with pressure (fig. 8(b)). As the pressure is increased, the peak of the damage rate curve is higher and narrower, and occurs earlier.

During the 3×10^5 N/m² test, a specimen failure occurred after 120 minutes. A second specimen was run, and the test continued for a total of 360 minutes. Because the cumulative volume loss of the two specimens run at the same pressure showed a difference of about 10 mm³ at the 120 minute point, separate curves are plotted in Fig. 8.

Fig. 8(b), shows that the volume-loss rates increase substantially after 240 minutes for the specimens tested at 3×10^5 and 4×10^5 N/m². This increase is most likely due to undercutting of the surface by cavitation and the resultant loss of large particles of material. Some large particles of specimen material were found in the sodium bath. Further

evidence of such undercutting is presented in the section dealing with the metallographic studies.

Volume loss data were also obtained for AISI 316 stainless steel and Stellite 6B at 427° C and at pressures of 1×10^5 , 2.7×10^5 , and 4×10^5 N/m². Increasing the test pressure increased the cumulative volume loss in each case, and both materials exhibited steady-state volume loss rates that increased with increasing pressure.

The steady-state volume loss rates discussed to this point are based on the conventional method of measuring cavitation damage by use of the total area exposed to cavitation. This method does not take into account changes in the damage pattern. From the macrographs of Fig. 9, it is obvious that there is an area of heavy damage, and a surrounding rim of little or no damage on the tested specimens. This heavily damaged area was reduced in diameter, but the depth of damage increased as pressure was increased. If the volume loss rate data are normalized on the basis of damaged area only, volume loss rate is found to vary as a power of pressure. Details of the normalizing process may be found in Ref. 32. The results of normalizing the steady-state volume loss rates of the three tested materials are shown in Fig. 10. Within the range of conditions considered in this investigation, it can be seen from Fig. 10 that the average volume loss rate can be expressed as a power of pressure above pressures of 2×10^5 N/m². The slopes of the curves for AISI 316 stainless

steel, L-605, and Stellite 6B are 1.6, 2.0, and 2.7, respectively. It should be noted, however, that in Fig. 10 the data points measured at $1 \times 10^5 \text{ N/m}^2$ tend to fall below extensions of the lines established by the higher pressure points. This can be explained by the fact that in theory cavitation damage must be zero at pressures approximately equal to the vapor pressure of the fluid. The value of vapor pressure is given in Fig. 10. On the logarithmic plot of Fig. 10, if the linear relationship held at the lower pressures (in the vicinity of $1 \times 10^5 \text{ N/m}^2$ and below), zero damage would be approached only at pressures very much lower than the vapor pressure. Therefore, the curves must fall away from the linear relationship toward the pressure axis at low pressure and this "fall off" apparently begins in the region of $1 \times 10^5 \text{ N/m}^2$.

The results of the present investigation differ from those obtained by previous investigators (ref. 33). Using a low-frequency (6500 Hz) magnetostrictive device in water, they found that for a given exposure time, damage increased with increasing pressure up to about $2 \times 10^5 \text{ N/m}^2$ and subsequently decreased as pressure was further increased. No damage was observed at $4 \times 10^5 \text{ N/m}^2$. It may be that because the apparatus used for the earlier tests (ref. 33) had a relatively low frequency resulting in relatively low specimen velocities, cavitation was reduced greatly at the higher ambient pressures. The high-frequency device used in the

present investigation is, however, capable of generating cavitation at these higher ambient pressures.

From Fig. 10, it is apparent that the three materials have the same relative ranking with respect to cavitation damage resistance at high pressures that they have at atmospheric pressure. Accelerated material damage tests, therefore, may be run at higher ambient pressures, and test time can be shortened by at least an order of magnitude, thereby allowing evaluation of a greater number of materials in a given time.

The Combined Effect of Temperature and Pressure of the Cavitating Liquid on Cavitation Damage

In engineering practice, the temperature of the cavitating fluid will often vary as well as the pressure. Therefore, it was considered desirable to determine the combined effects of temperature and pressure on cavitation damage. L-605, the moderately damage resistant alloy was chosen for this phase of the investigation. This was done to accommodate the possible wide variations in damage that could result from changes in the characteristics of the cavitating fluid with temperature.

The cavitation damage observed with L-605 at 1×10^5 , 2×10^5 , 3×10^5 , and 4×10^5 N/m² is shown in terms of volume loss at 204^o, 427^o, and 649^o C in Fig. 11. Volume loss rates were also calculated and are plotted in Fig. 12. Details of this phase of the investigation can be found in Ref. 27. At each temperature considered, cavitation at higher pressures

resulted in (1) higher cumulative volume loss, (2) a higher volume loss rate peak, and (3) a higher level of average volume-loss rate. The average volume-loss rate was used as an objective measure of steady-state volume loss rate and is defined for this series of tests as the average volume-loss rate observed between 120 minutes and the termination of the test. Further discussion on the validity of methods of evaluating rate curves can be found in Ref. 29, and the discussion to Ref. 34. After 120 minutes, the volume-loss rate for all pressure levels except for the $1 \times 10^5 \text{ N/m}^2$ tests had passed through a peak and the volume loss rate did not change significantly over an extended period of time. Although the $1 \times 10^5 \text{ N/m}^2$ tests did not pass beyond a peak, the damage rates were very low and consistent. Therefore, the highest rate at this low pressure was used instead of the average volume loss rate. The volume loss rate data were then normalized (as in the preceding section) by multiplying the volume loss rate by the ratio of the total specimen area to the heavily damaged area. In this manner, the intensive effects of temperature and pressure on volume loss rate were determined independently of the size of the damaged area. The normalized cavitation damage data are plotted in Figs. 13 to 15. The average volume loss rates in Fig. 13 for the several constant test temperatures can be expressed as powers of pressure above a pressure of $2 \times 10^5 \text{ N/m}^2$. Exponents of 1.6, 1.9, and 1.7 were measured

for the lines fitted to the 204^o, 427^o, and 649^o C data between 2×10^5 and 4×10^5 N/m².

Fig.14 shows the effect of temperature on cavitation damage at four different pressures. The maximum normalized volume loss rates were observed at 427^o C for all test pressures. The true shapes of these curves only can be conjectured, however, because many different curves can be drawn through three points. More experimental data are needed to define completely the shapes of the curves for this figure. This shape of curve, however, is consistent with that of other investigators using aqueous solutions as the testing medium (ref. 35). The peaking is believed to be due, in theory, to two factors:

- (1) At very low temperatures nucleation of cavities is difficult, and a reduced number of cavities are produced.
- (2) At very high temperatures, great numbers of cavities are produced but their impact force is lessened by possible "cushioning effects," and the fact that a smaller difference exists between ambient pressure and the vapor pressure of the fluids.

The cavitation damage rates at 1×10^5 N/m² were not in the same order with respect to temperature as the rates measured at higher pressures. Damage was least at 649^o C at 1×10^5 N/m² but for 2×10^5 , 3×10^5 , and 4×10^5 N/m² it was least at 204^o C. Other factors such as varying solubility of argon in sodium with temperature and pressure

may contribute to these differences.

To help visualize the combined effects of temperature and pressure of the cavitating fluid on cavitation damage, Fig. 15 was constructed. This figure is an average volume-loss rate contour diagram with temperature and pressure as the axes. The two theoretically limiting curves for zero cavitation damage rate are the solid-liquid and liquid-vapor curves. It is believed that as pressure increases, the constant volume-loss rate contours may close again due to the suppression of cavitation by high pressures. However, due to power limitations of the test facility, pressures above $4 \times 10^5 \text{ N/m}^2$ were not investigated.

The quantitative values of damage shown in Fig. 15 obviously would be different for different types of test facilities and for different test amplitudes and frequencies because damage is dependent on the amount of cavitation generated; however, the general trend of increasing damage with increasing pressure is valid. Further tests at other temperatures and higher pressures are needed to determine the combination of temperature and pressure that would cause maximum cavitation damage with this facility for L-605 as well as for other materials.

Relation Between Accelerated Cavitation Damage and Material Properties

The ability to predict which materials have superior resistance to cavitation damage from mechanical property data would obviously be useful.

Thus, a method of correlating cavitation damage with readily available material properties, even though empirical in nature, might serve as a guide to designers and as a substitute for accelerated cavitation tests.

One of the attempts to predict the ranking of materials with respect to cavitation damage resistance in liquid metals (refs. 18 and 20) indicates that the severity of cavitation damage may be inversely related to the strain energy of materials. Strain energy is approximately equivalent to the area beneath the stress-strain curve. When the stress-strain curves are not available, strain energy can be approximated by the following equation:

$$S.E. = \frac{Y.S. + T.S.}{2} e$$

where

Y.S. = yield strength

T.S. = tensile strength

e = elongation

The necessary properties for calculating the strain energy of materials at 427^o C are given in Table 3; Fig. 16 shows the relation between strain energy and the reciprocal of the steady-state volume loss rate of materials subjected to cavitation damage in sodium. The volume loss rate values were obtained from Fig. 5(a) at 4 hours except that of Stellite 6B which was taken from data extended to 10 hours to insure a steady-

state rate. The exact shape of the volume loss rate curve for L-605 is not certain, as was mentioned previously. Although this material may not have reached a steady-state condition after 4 hours, the value for loss rate at this test time was used as an approximation of the steady-state rate.

Fig. 16 shows that most of the data falls close to a straight line; however, the data point for the material that performed most favorably, Stellite 6B, is very far removed from the data of the other materials. Thus, the use of the strain energy parameter would have resulted in omitting from consideration one of the most cavitation damage resistant materials. Several suggestions for this apparent anomaly are mentioned in the discussion to Ref. 36.

Evidently strain energy alone is not entirely representative of the properties that control the resistance of a material to cavitation damage. Some modifications of the strain energy concept are given in Ref. 37. The hardness, elastic modulus, and fatigue limit are other readily measurable material properties that might be expected to have some effect on cavitation damage resistance, but there have nearly always been exceptions to every correlation attempt. In order to completely evaluate their role singly or in combination, extensive additional data for many materials are needed. Finally, the validity of any such parameter would be affected by corrosion variables that differ for different environments and that

might, in some cases, be overriding. In any event, much additional research is needed to achieve a better understanding of the relations between resistance to cavitation damage and readily measurable material properties.

Metallurgical Aspects of Cavitation Damage

Extensive metallographic studies were made to shed light on the nature of material damage induced by cavitation. Cavitation damage to materials was examined in two different ways: First, the specimen surface was repeatedly examined during the early stages of testing; second, after a test was completed, specimens were cross cut (axially sectioned) to study the nature of the material damage resulting from long time cavitation exposure. Both high and low magnification studies were made. A summary of the major findings is presented in the following sections.

Comparison of damage to structure in sodium and mercury. -

Macrographs of all the materials subjected to cavitation damage in sodium for 4 hours at 427⁰ C are shown in Fig. 17. The alloys can be arbitrarily separated into three groups, each displaying a different degree of cavitation damage: (1) severe damage - annealed Sicromo 9M, (2) intermediate damage - AISI type 316 stainless steel and 318 stainless steel, Inconel 600, A-286, and Hastelloy X, and (3) slight damage - L-605, René 41, and Stellite 6B.

Macrographs of many of these materials after being subjected to cavitation damage in mercury are shown in Fig. 18. Again, these materials can be separated by visual observation into three groups: (1) severe damage - annealed Sicromo 9M and Hastelloy X, (2) intermediate damage - hardened Sicromo 9M and L-605, and (3) slight damage - Stellite 6B. It is apparent that some of the materials such as L-605 and Hastelloy X can be grouped in a more severe damage category after exposure in mercury. Comparison of Figs. 17 and 18 also illustrates a marked difference between damage patterns caused by sodium and those caused by mercury. After testing in sodium, the specimen surfaces were more finely textured, and the rims of the specimens were relatively undamaged. After testing in mercury the specimen surfaces were very rough and deeply cratered with heavy damage occurring near the rim. These differences in surface damage probably resulted from differences in the nature of the fluid flow for each test medium and from differences in liquid impact forces resulting from the widely dissimilar properties of sodium and mercury, primarily density and surface tension.

Photomicrographs of surfaces of specimens tested in sodium for only 5 minutes are shown in Fig. 19. All specimens showed a selective damage pattern. Three specific examples are shown in the figure. AISI type 316 stainless steel showed severe matrix attack after only 5 minutes while some grain or twin boundaries stood out in relief. On the other hand, in

L-605 both grain and twin boundaries were attacked more heavily than the matrix. Stellite 6B, the most resistant material, showed very slight matrix attack after 5 minutes with carbide particles in relief. A few carbide particles were, however, dislodged in the early phases of test. As test time was increased, more carbide particles were dislodged, leaving deep pits. These pits which widened with time, evidently served as sites for increased cavitation attack of the matrix. These photomicrographs indicate that although some of the carbide particles were dislodged, most of them remained intact, and their presence evidently is a major factor in making Stellite 6B so highly resistant to cavitation damage. In mercury, no particular portion of the microstructure of any of the materials except Stellite 6B appeared to be attacked preferentially (fig. 20). As in the case of the sodium tested specimens, the carbide particles in Stellite 6B were found to be particularly resistant to cavitation attack by mercury; whereas, the softer matrix showed definite attack.

Subsurface effects. - After the tests were completed, specimens of AISI 316 stainless steel, L-605, and Stellite 6B were cross sectioned to study the effect of cavitation damage below the surface of the material. Fig. 21 shows photomicrographs of these specimens after exposure to cavitation in sodium at 427° C and at the highest fluid pressure considered, 4×10^5 N/m². All three materials exhibited undercutting and transgranular cracking. Evidence of some subsurface deformation existed in the form

of slip bands for all materials. Breaking of subsurface carbides in Stellite 6B is apparent in Fig. 19(c). Specimens of the same materials were also sectioned after exposure to cavitation at 427⁰ C under the lower pressure of 1×10^5 N/m². Although damage at the lower pressure required much longer times than at higher pressure, similar damage characteristics were observed at both pressures.

Relative influence of chemical and mechanical effects on cavitation damage. - No evidence of any chemical reaction zone was found in the cavitation damaged regions of any specimen we tested either in mercury or sodium. This is of extreme interest since the role of corrosion in cavitation damage relative to mechanical effects has always been a point of considerable discussion (ref. 38). From our studies, it is possible to make an additional comparison; namely, the cavitation damage experienced by materials in sodium with that observed after cavitation in water (ref. 39). In one of our investigations (ref. 39), we studied the cavitation damage experienced by several pure metals and a nickel-base superalloy in water. Fig. 22 shows the results of cavitation damage to two of these materials, iron and tantalum. Undercutting and transgranular cracking were clearly evident in these materials, and to a lesser extent, some subsurface deformation was noted. This similarity in damage characteristics of materials tested in water and in sodium, coupled with the fact that no reaction zones were noted in either case, lends credence

to the view that cavitation damage obtained in the ultrasonic vibratory tests is primarily mechanical in nature rather than chemical.

Ultrasonic Vibratory Testing Applied as Etching Technique

An interesting feature was noted in this investigation which may have considerable application as a metallographic technique. We found that the selective attack resulting from the ultrasonic vibratory technique of creating accelerated cavitation damage is effective in revealing microstructural features (ref. 40). Fig. 23 is a replica electron micrograph of a cavitation damaged specimen of the nickel-base alloy, Udimet 700. It clearly shows the features typical of this gamma prime strengthened superalloy. The structure was revealed by exposing a Udimet 700 specimen to accelerated cavitation damage in the ultrasonic vibratory apparatus for 120 minutes in water. The flagstone appearance of the gamma prime phase is clearly apparent. The appearance of this specimen suggests that accelerated cavitation damage achieved in the manner described may be extremely useful as a technique for selective etching of materials. The weaker phases would be removed, leaving the tougher, harder, more impact resistant phases. This method would also allow the investigator to easily recover material from the distilled water (or any other fluid desired) for further analysis without the disadvantages associated with the use of reactive chemicals. Quite apart from the principal objectives of our investigation, this result is considered to be an important by-product. It is

pointed out for the benefit of those who are concerned with the metallographic aspects of materials investigations.

SUMMARY OF RESULTS

The resistance to cavitation damage of a wide variety of candidate materials for components of liquid metal space power conversion systems was investigated in sodium and mercury. A magnetostrictive-type apparatus was used to achieve accelerated cavitation damage. The combined effects of temperature and pressure on damage were investigated. Metallographic studies were made to determine the nature of cavitation damage.

1. In all cases, the materials that were tested in both sodium and mercury ranked in the same order with respect to resistance to cavitation damage. Stellite 6B, a hard, wear-resistant cobalt-base alloy, was far superior to all other materials investigated in both fluids. The relatively soft, iron-base alloy, annealed Sicromo 9M, had the lowest resistance to cavitation damage.

2. The severity of the cavitation damage experienced by all materials in mercury at 149°C was consistently greater (by factors of 2 to 7 times) than that experienced by the same materials in sodium at 427°C .

3. Surface roughness measurements provided a ranking of materials with respect to cavitation damage resistance similar to that obtained from the usual volume loss measurements.

4. Visual observations of pump impeller blades of AISI types 316 and

318 stainless steels, and René 41 operated under cavitating conditions for 250 hours at temperatures up to 816° C in sodium indicated the same ranking of these materials with regard to cavitation damage resistance as that determined in the accelerated laboratory cavitation tests. The nickel-base alloy, René 41, showed considerably less damage than either of the steels.

5. At constant fluid temperature, increasing pressure on the cavitating fluid significantly increased cavitation damage to all materials. When the material volume-loss rate data were normalized to include only the heavily damaged area of the specimens, the steady-state volume-loss rate increased as a power function of pressure at pressures above approximately 2×10^5 N/m². The exponents ranged from 1.6 to 2.7, depending on the material. The fact that increasing fluid pressure increased cavitation damage implies that in fluid systems where cavitation occurs in high-pressure regions, damage to components may be much greater than would normally be expected from conventional laboratory cavitation tests conducted at atmospheric pressures.

6. The relative ranking of the materials with respect to resistance to cavitation damage was the same at all pressures of the cavitating fluid. This result, together with the fact that the damage rate increases with increasing pressure, suggests that a greater number of materials may be

evaluated in the laboratory in a given time at higher pressures than at atmospheric pressure.

7. The combined effect of temperature and pressure on cavitation damage to L-605 has been shown in terms of volume loss rate normalized to consider only the heavily damaged area of the specimens. Volume loss rate increased as a power function of pressure above $2 \times 10^5 \text{ N/m}^2$ with the exponents of 1.6, 1.9, and 1.7 for test temperatures of 204° , 427° , and 649° C , respectively. For each pressure considered, damage was maximum at the intermediate temperature of 427° C .

8. Metallographic examination at high magnifications during the early stages of cavitation damage indicated that cavitation in sodium resulted in non-uniform damage to all materials, as evidenced by the delineation of twin and grain boundaries. Cavitation in mercury, on the other hand, resulted in a uniformly damaged surface with no apparent preferential attack except for Stellite 6B, by far, the most damage-resistant material. In this alloy, the carbides were more resistant than the matrix. Macroscopic examination of all materials after appreciable damage had occurred indicated that cavitation in sodium resulted in a fine-textured (matte) surface; whereas, exposure to mercury resulted in very coarse, deep craters.

9. Upon completion of cavitation testing, metallographic examination of axially sectioned specimens usually revealed severe undercutting of the surface and transgranular cracking. Subsurface deformation was indicated

in all materials by the appearance of slip bands. The same damage characteristics were observed in materials subjected to cavitation damage in distilled water. The similarity of damage characteristics tends to indicate that cavitation damage in accelerated tests is primarily mechanical rather than chemical in nature.

10. The selective attack resulting from the ultrasonic vibratory method of creating accelerated cavitation damage was effective in revealing microstructural features. This suggests that this technique may be useful as a means of etching in metallographic studies.

REFERENCES

1. Kulp, Robert S. ; and Altieri, James V. : Cavitation Damage of Mechanical Pump Impellers Operating in Liquid Metal Space Power Loops. NASA CR-165, 1965.
2. Smith, P. G. ; DeVan, J. H. ; and Grindell, A. G. : Cavitation Damage to Centrifugal Pump Impellers During Operation With Liquid Metals and Molten Salt at 1050 - 1400 F. J. Basic Eng. , vol. 85, no. 3, Sept. 1963, pp. 329-337.
3. Hammitt, F. G. : Observations on Cavitation Damage in a Flowing System. J. Basic Eng. , vol. 85, no. 3, Sept. 1963, pp. 347-359.
4. Anon. : Sunflower Power Conversion System. Rep. ER-5163, Thompson Ramo Wooldridge, Inc. (NASA CR-56206), 1962.
5. Anon. : SNAP-8 Topical Materials Report for 1963. Vol. II. Rep. 2822 (Special), Aerojet-General Corp. , Mar. 1964.
6. Knapp, R. T. ; and Hollander, A. : Laboratory Investigations of the Mechanism of Cavitation. Trans. ASME, vol. 70, no. 5, July 1948, pp. 419-435.

7. Preiser, H. S. ; and Tytell, B. H. : The Electrochemical Approach to Cavitation Damage and its Prevention. *Corrosion*, vol. 17, no. 11, Nov. 1961, pp. 107-121.
8. Heyman, F. J. : Erosion by Cavitation, Liquid Impingement, and Solid Impingement. A Review. Rep. E-1460, Westinghouse Electric Corp., Mar. 15, 1968.
9. Plesset, M. S. ; and Ellis, A. T. : On the Mechanism of Cavitation Damage. *Trans. ASME*, vol. 77, no. 7, Oct. 1955, pp. 1055-1064.
10. Plesset, Milton S. : Pulsing Technique for Studying Cavitation Erosion of Metals. *Corrosion*, vol. 18, no. 5, May 1962, pp. 181-188.
11. Naudé, Charl F. ; and Ellis, Albert T. : On the Mechanism of Cavitation Damage by Nonhemispherical Cavities Collapsing in Contact With a Solid Boundary. *J. Basic Eng.*, vol. 83, no. 4, Dec. 1961, pp. 648-656.
12. Wheeler, W. H. : Indentation of Metals by Cavitation. *J. Basic Eng.*, vol. 82, no. 1, Mar. 1960, pp. 184-194.
13. Lichtman, J. Z. ; and Weingram, E. R. : Cavitation Design Handbook. Rep. NR 062-314, U. S. Naval Applied Science Lab., Sept. 30, 1964.
14. Hammitt, F. G. ; Barinka, L. L. ; Robinson, M. J. ; Pehlke, R. D. ; and Siebert, C. A. : Initial Phases of Damage to Test Specimens in a Cavitating Venturi. *J. Basic Eng.*, vol. 87, no. 2, June 1965, pp. 453-464.
15. Leith, W. C. ; and Thompson, A. Lloyd: Some Corrosion Effects in Accelerated Cavitation Damage. *J. Basic Eng.*, vol. 82, no. 4, Dec. 1960, pp. 795-807.

16. Anon. : Erosion by Cavitation or Impingement. Spec. Tech. Publ. 408, ASTM, 1967.
17. Anon. : Characterization and Determination of Corrosion Resistance. Spec. Tech. Publ. 474, ASTM, 1970.
18. Thiruvengadam, A. : A Unified Theory of Cavitation Damage. J. Basic Eng. , vol. 85, no. 3, Sept. 1963, pp. 365-376.
19. Hammitt, F. G. : Cavitation Damage and Performance Research Facilities. Symposium on Cavitation Research Facilities and Techniques. J. William Holl and Glenn M. Wood, eds. , ASME, 1964, pp. 175-184.
20. Preiser, H. S. ; Thiruvengadam, A. ; and Couchman, C. : Cavitation Damage Research Facilities for High Temperature Liquid Alkali Metal Studies. Symposium on Cavitation Research Facilities and Techniques. J. William Holl and Glenn M. Wood, eds. , ASME, 1964, pp. 146-156.
21. Kelly, R. W. ; Wood, G. M. ; Marman, H. V. ; and Milich, J. J. : Rotating Disk Approach for Cavitation Damage Studies in High-Temperature Liquid Metal. Paper 63-AHGT-26, ASME, Mar. 1963.
22. Chao, C. ; Hammitt, F. G. ; King, C. L. ; and Rogers, D. O. : ASTM Round-Robin Test With Vibratory Cavitation and Liquid Impact Facilities of 6061-T 6511 Aluminum Alloy, 316 Stainless Steel, and Commercially Pure Nickel. Rep. MMPP-344-3-T, 01356-4-T, Univ. Michigan, Nov. 1968.
23. Young, Stanley G. : Cavitation Damage of Stainless Steel, Nickel, and an Aluminum Alloy in Water for ASTM Round Robin Tests. NASA TM X-1670, 1968.
24. Young, Stanley G. ; and Johnston, James R. : Accelerated Cavitation Damage of Steels and Superalloys in Liquid Metals. NASA TN D-3426, 1966.

25. Robinson, L. E. ; Holmes, B. A. ; and Leith, W. C. : Progress Report on Standardization of the Vibration-Cavitation Test. Trans. ASME, vol. 80, no. 1, Jan. 1958, pp. 103-107.
26. Hobbs, J. M. ; Laird, A. ; and Brunton, W. C. : Laboratory Evaluation of the Vibratory Cavitation Erosion Test. Rep. NEL-271, National Engineering Lab. , Glasgow, Jan. 1967.
27. Young, Stanley G. ; and Johnston, James R. : Effect of Temperature and Pressure on Cavitation Damage to a Cobalt-Base Alloy in Sodium. NASA TN D-5273, 1969.
28. Thiruvengadam, A. ; and Preiser, H. S. : On Testing Materials for Cavitation Damage Resistance. Tech. Rep. 233-3, Hydronautics, Inc. , Dec. 1963. (Available from DDC as AD-600016.)
29. Heymann, F. J. : On the Time Dependence of the Rate of Erosion Due to Impingement on Cavitation. Erosion by Cavitation or Impingement. Spec. Tech. Publ. 408, ASTM, 1967, p. 70.
30. Plesset, Milton S. ; and Devine, Robert E. : Effect of Exposure Time on Cavitation Damage. Rep. 85-31, California Inst. Tech. , Aug. 1965. (Available from DDC as AD-471191.)
31. Cunnann, Walter S. ; and Reemsnyder, Dean C. : Cavitation Damage and the Effect of Fluid Temperature on the Performance of an Axial-Flow Pump in Liquid Sodium. NASA TN D-5484, 1969.
32. Young, Stanley G. ; and Johnston, James R. : Effect of Cover Gas Pressures on Accelerated Cavitation Damage in Sodium. NASA TN D-4235, 1967.

33. Peters, H. ; and Rightmire, B. G. : Cavitation Study by the Vibratory Method. Proceeding of the Fifth International Congress for Applied Mechanics. J. P. Den Hartog and H. Peters, eds. , John Wiley & Sons, Inc. , 1939, pp. 614-616.
34. Young, S. G. ; and Johnston, J. R. : Effect of Temperature and Pressure on Cavitation Damage in Sodium. Characterization and Determination of Corrosion Resistance. Spec. Tech. Publ. 474, ASTM, 1970, pp. 67-108.
35. Devine, Robert E. ; and Plesset, Milton S. : Temperature Effects in Cavitation Damage. Rep. 85-27. California Inst. Tech. , Apr. 1964. (Available from DDC as AD-438223.)
36. Young, S. G. ; and Johnston, J. R. : Accelerated Cavitation Damage of Steels and Superalloys in Sodium and Mercury. Erosion by Cavitation or Impingement. Spec. Tech. Publ. 408, ASTM, 1967, pp. 186-219.
37. Thiruvengadam, A. : The Concept of Erosion Strength. Erosion by Cavitation or Impingement. Spec. Tech. Publ. 408, ASTM, 1967, pp. 22-41.
38. Schulmeister, R. : Vibratory Tests in Water on the Combined Action of Cavitation and Corrosion. Characterization and Determination of Corrosion Resistance. Spec. Tech. Publ. 474, ASTM, 1970, pp. 109-126.
39. Young, Stanley G. : Study of Cavitation Damage to High-Purity Metals and a Nickel-Base Superalloy in Water. NASA TN D-6014, 1970.
40. Young, Stanley G. : Etching of Metallographic Specimens by Cavitation. Presented at the Third Annual Meeting of the International Metallographic Society, Inc. , Cleveland, Ohio, Nov. 16-18, 1970.

TABLE 1. - NOMINAL CHEMICAL COMPOSITIONS OF TEST MATERIALS

Material	Composition, weight percent														
	Iron	Nickel	Cobalt	Chromium	Molybdenum	Tungsten	Columbium	Titanium	Aluminum	Carbon	Manganese	Silicon	Phosphorous	Sulfur	Other
Stellite 6B ^b	a ₃	a ₃	Bal.	30	a _{1.5}	4.5	---	---	---	1.1	a ₂	a ₂	---	---	---
René 41 (AMS 5712) ^c	a ₅	Bal.	10 to 12	18 to 20	9 to 10.5	---	---	3 to 3.3	1.4 to 1.8	a _{0.12}	a _{0.10}	a _{0.50}	---	a _{0.015}	0.003 to 0.01 (boron)
L-605 (AMS 5759 B) ^c	a ₃	9 to 11	Bal.	19 to 21	---	14 to 16	---	---	---	0.05 to 0.15	1 to 2	a _{1.0}	a _{0.04}	a _{0.03}	---
Hastelloy X (AMS 5754 D) ^c	17 to 20	Bal.	0.5 to 2.5	20.5 to 23	8 to 10	0.2 to 1.0	---	---	---	0.05 to 0.15	a _{1.0}	a _{1.0}	a _{0.04}	a _{0.03}	---
A-286 (AMS 5736 B) ^c	Bal.	24 to 27	---	13.5 to 16	1 to 1.5	---	---	1.9 to 2.3	a _{0.35}	a _{0.08}	1 to 2	0.4 to 1	0.04	0.03	0.003 to 0.01 (boron) 0.1 to 0.5 (vanadium)
Inconel 600 (AMS 5665 G) ^c	6 to 10	Bal.	a ₁	14 to 17	---	---	a ₁	a _{0.5}	a _{0.35}	a _{0.15}	a _{1.0}	a _{0.5}	---	a _{0.015}	a _{0.5} (copper)
AISI 318 stainless steel ^d	Bal.	13 to 15	---	17 to 19	2 to 2.75	---	0.8 (min)	---	---	a _{0.08}	a _{2.5}	a _{1.0}	---	---	---
AISI 316 stainless steel (AMS 5648 C) ^c	Bal.	12 to 14	---	17 to 19	2 to 3	---	---	---	---	0.08	1.25 to a _{2.0}	a _{1.0}	a _{0.04}	a _{0.03}	a _{0.50} (copper)
Sicromo 9M ^e	Bal.	---	---	8 to 10	0.9 to 1.2	---	---	---	---	a _{0.2}	0.35 to 0.65	a _{1.0}	a _{0.04}	a _{0.04}	---

^aMaximum.

^bAnon., "Wear Resistant Alloys," Bulletin No. F30-1-33-A, Haynes Stellite Co., 1962.

^cAMS Specifications, "René 41-AMS 5712; L605-AMS 5759 B; Hastelloy X - AMS 5754 D; A286-AMS 5736 B; Inconel-AMS 5665 G; and Type 316 Stainless Steel - AMS 5648 C."

^dAnon., "Stainless Steel Handbook," Allgheny Lumlum Steel Corp., 1951.

^eAnon., "High Alloy Castings," Bulletin No. 261, Duralloy Co., 1961.

TABLE 2. - HEAT TREATMENTS AND DENSITIES
OF TEST MATERIALS

Material	Heat treatment	Density, g/cm ³
Stellite 6B	Solution-heat treated at 1232 ^o C; air cooled	8.38
René 41	Solution-heat treated at 1079 ^o C; rapid quenched	8.25
L-605	Solution-heat treated at 1232 ^o C; water quenched	9.13
Hastelloy X	Solution-heat treated at 1177 ^o C; rapid air cooled	8.23
A-286	Solution-heat treated at 982 ^o C; water quenched; aged at 718 ^o C for 16 hr	7.94
Inconel 600	Annealed	8.43
AISI 318 stainless steel	Annealed	7.99
AISI 316 stainless steel	Annealed	7.98
Sicromo 9M	Annealed; heat treated at 954 ^o C for 1 hr, then at 732 ^o C for 1 hr; air cooled	7.61

TABLE 3. - MECHANICAL PROPERTIES AT 427⁰ C OF MATERIALS
USED FOR STRAIN ENERGY CALCULATIONS

Material	Ultimate tensile strength, MN/m ²	Yield strength, MN/m ²	Elongation, percent
Stellite 6B ^a	950	490	29
L-605 ^b	820	250	76
Hastelloy X ^b	690	320	50
A-286 ^b	940	630	21
Inconel 600 ^b	610	200	49
AISI 316 stainless steel ^b	480	190	40

^aAnon., "Wear Resistant Alloys," Bulletin No. F30-1-33-A, Haynes Stellite Co., 1962.

^bV. Weiss and J. G. Sessler, eds., "Aerospace Structural Metals Handbook," Syracuse University Press, 1963.

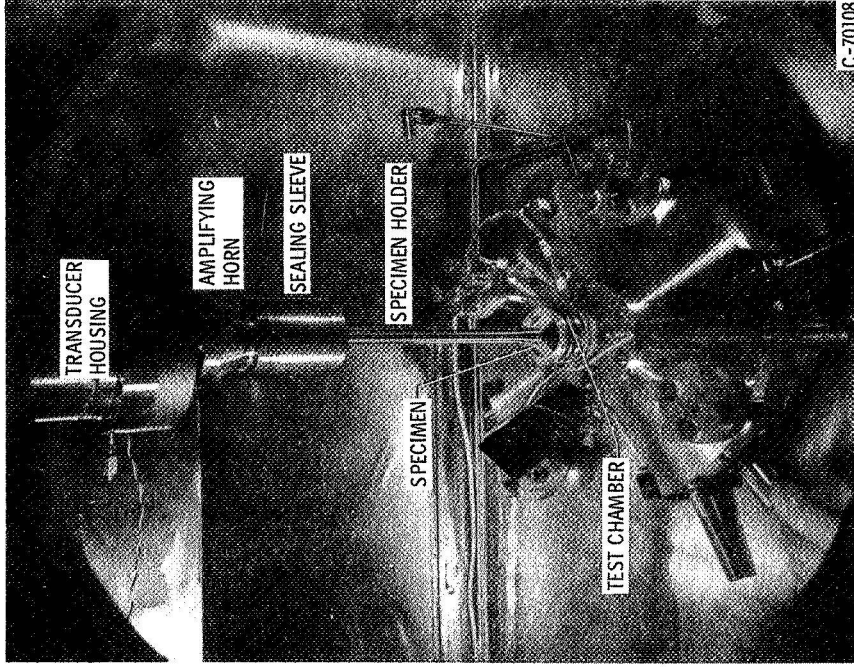


Figure 2. - Components of transducer assembly and liquid metal test chamber.

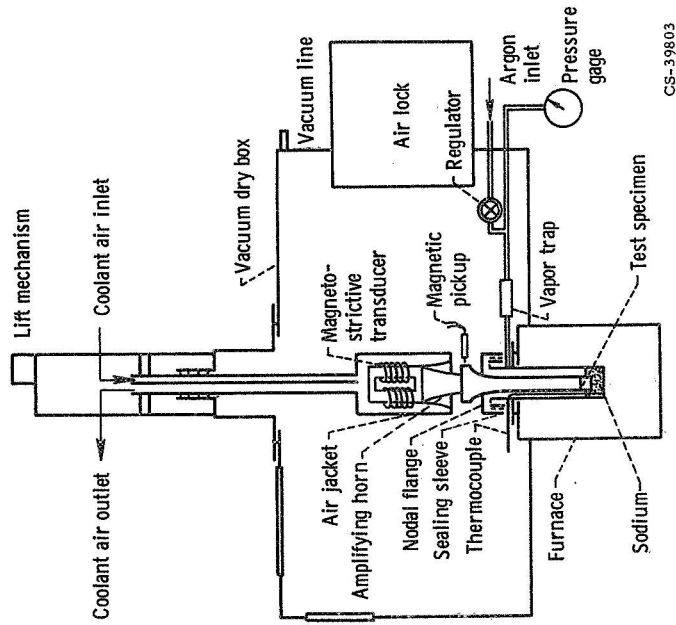


Figure 1. - Schematic diagram of cavitation apparatus.

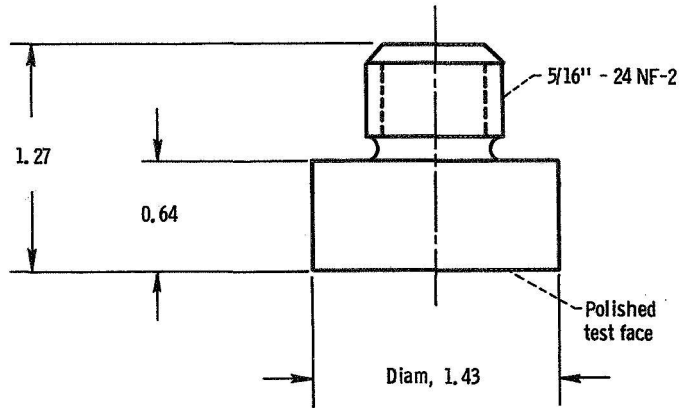


Figure 3. - Cavitation test specimen. (Dimensions in cm).

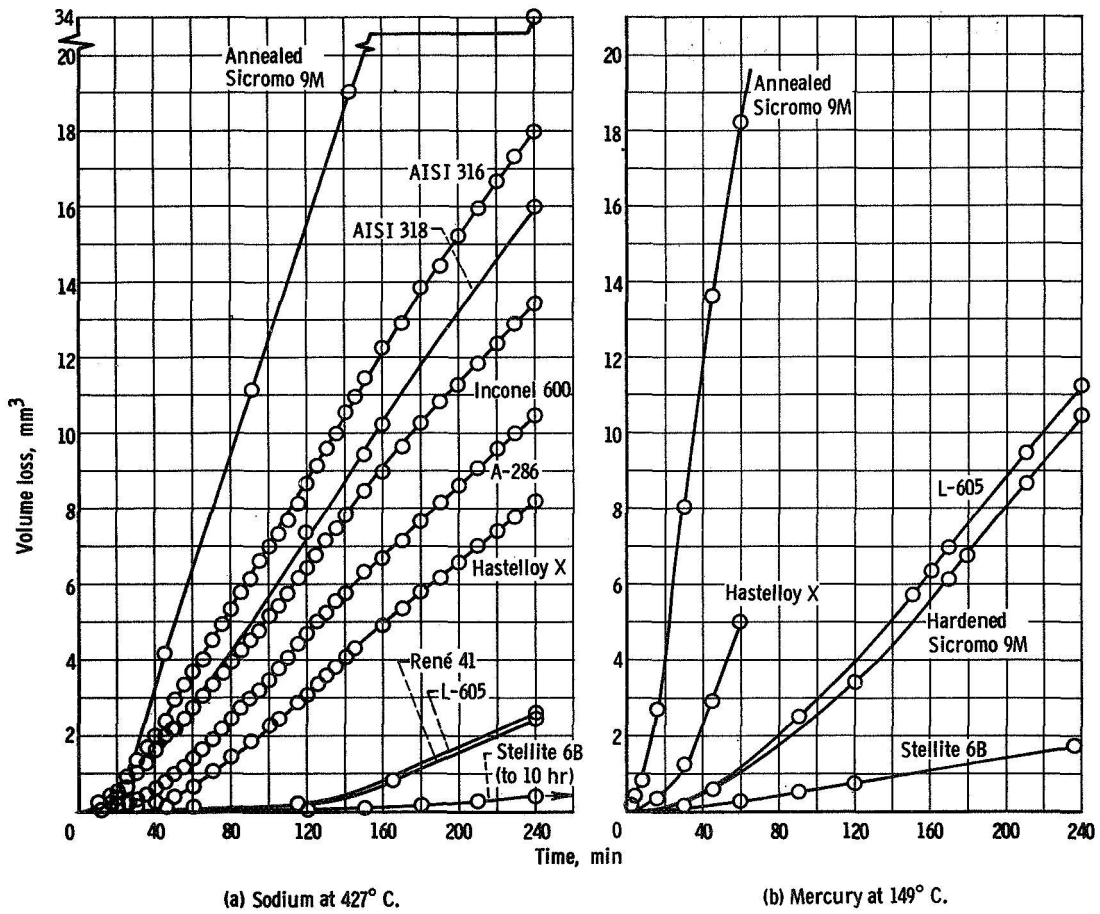
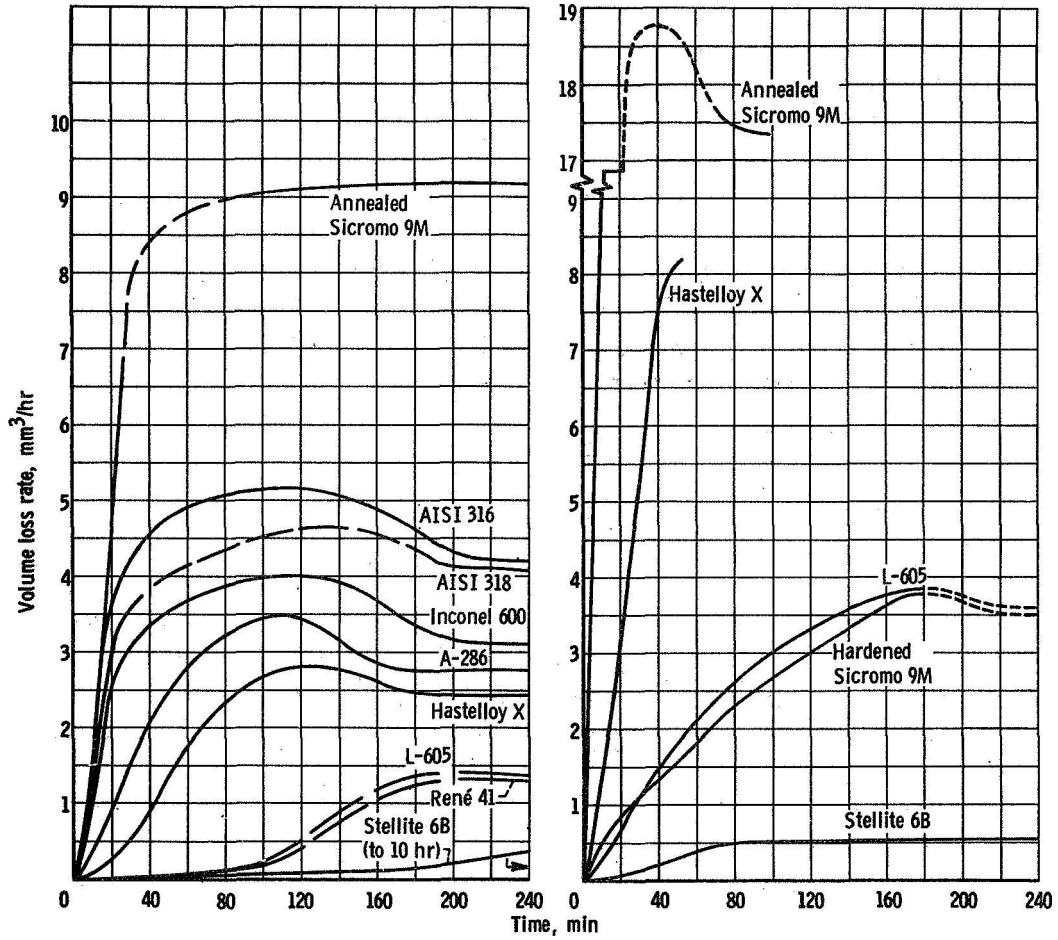


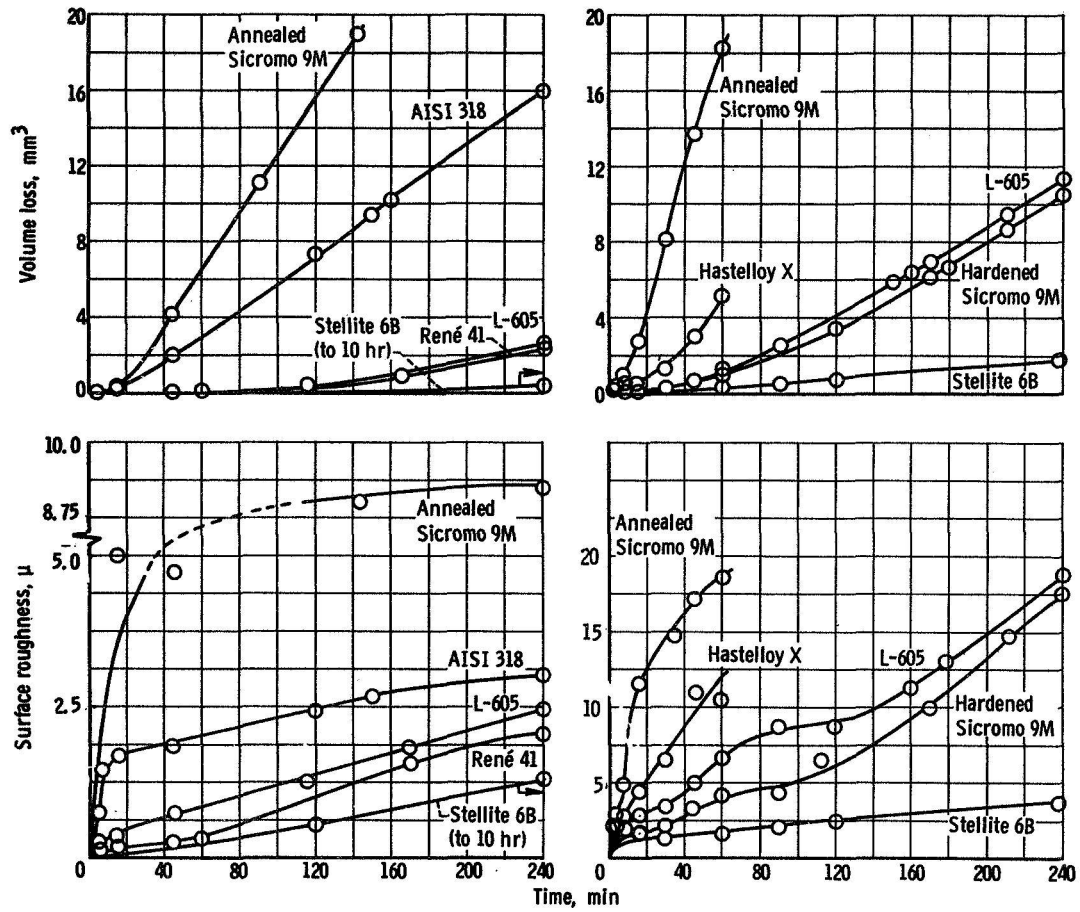
Figure 4. - Cavitation damage of materials in liquid metals.



(a) Sodium at 427°C .

(b) Mercury at 149°C .

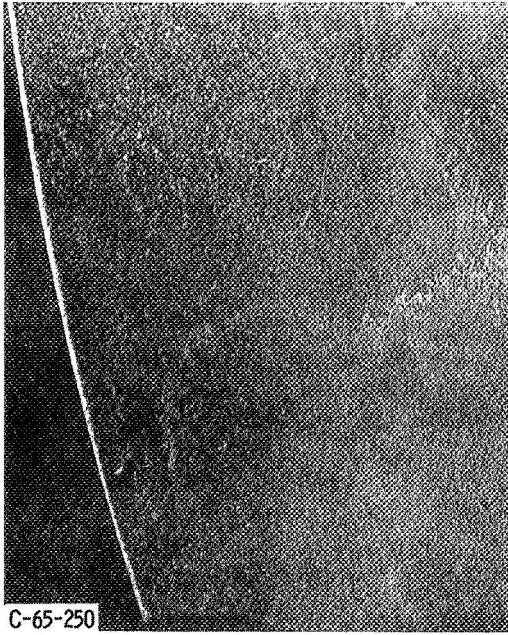
Figure 5. - Rate of cavitation damage of materials in liquid metals.



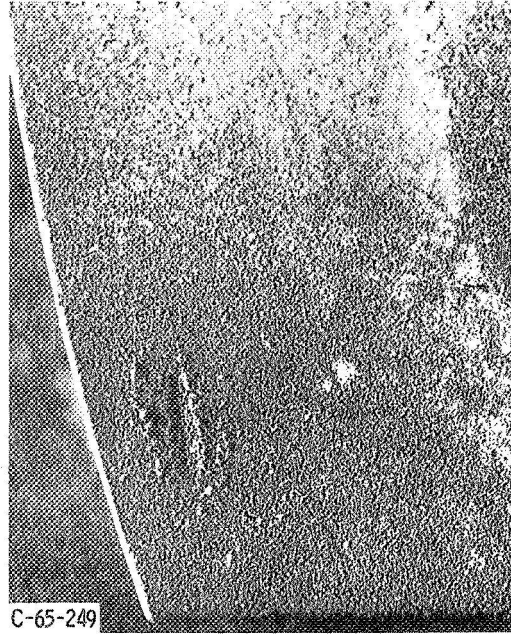
(a) Sodium at 427° C.

(b) Mercury at 149° C.

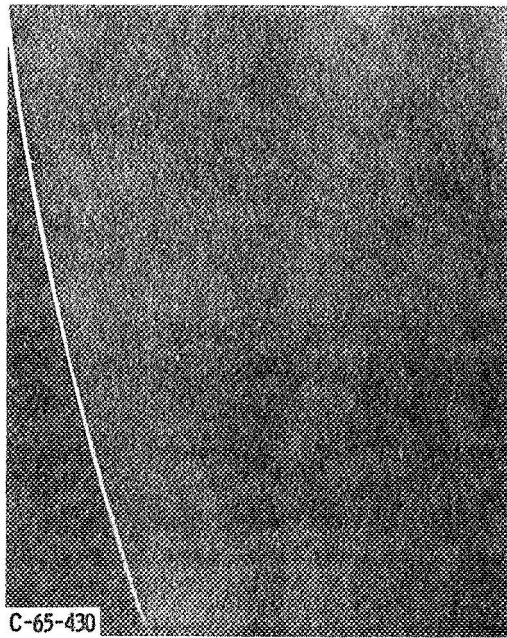
Figure 6. - Comparison of surface roughness and volume loss for alloys exposed to cavitation in liquid metals.



AISI 316 stainless steel



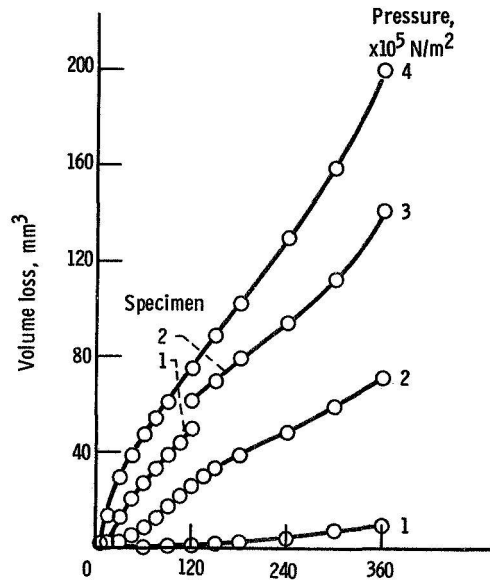
AISI 318 stainless steel



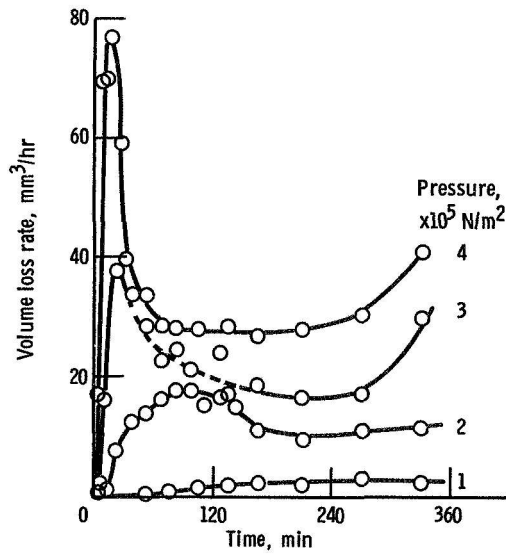
Rene 41

2.5 mm

Figure 7. - Cavitation damage to pump impeller blades operated in liquid sodium for 250 hr up to 816° C.



(a) Cumulative cavitation damage.



(b) Rate of cavitation damage.

Figure 8. - Cavitation damage of L-605 specimens tested in 427° C sodium at various pressures.

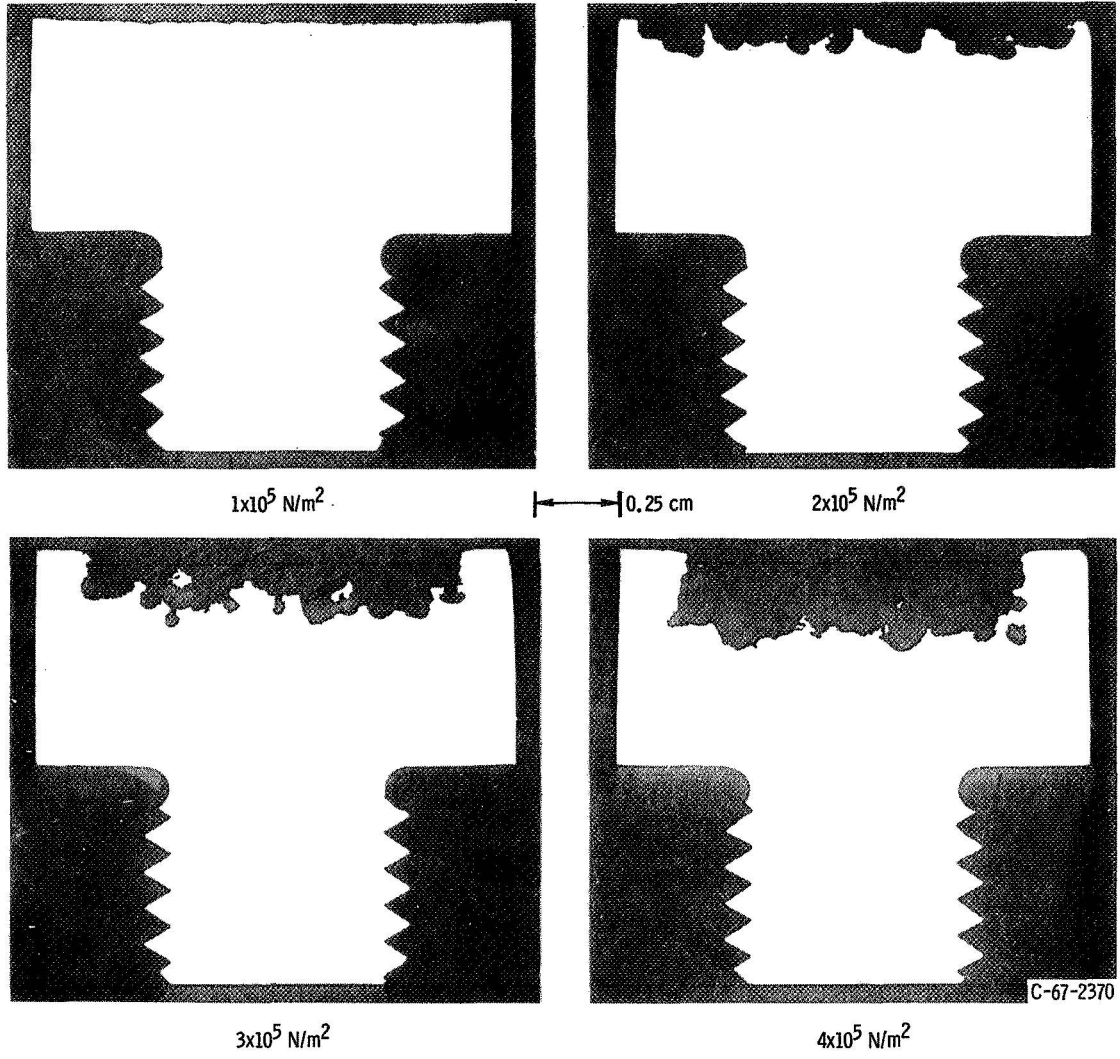


Figure 9. - Sections of L-605 specimens after exposure to cavitation in sodium at 427° C for 360 min at various pressures (unetched).

	Material	Slope
○	316 SS	1.6
△	L-605	2.0
□	6B	2.7

Vapor pressure at 427° C = $(1.0 \times 10^2 \text{ N/m}^2)$

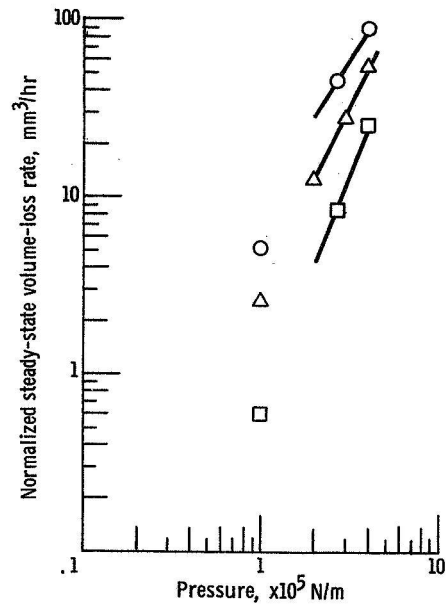
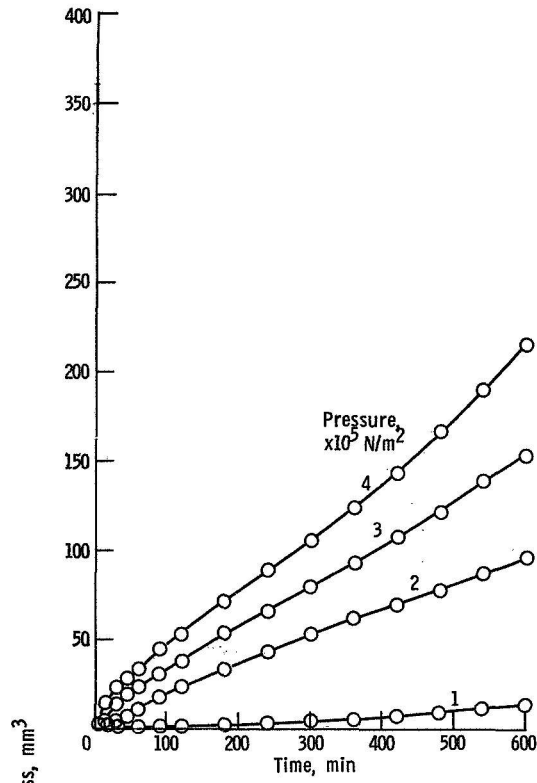
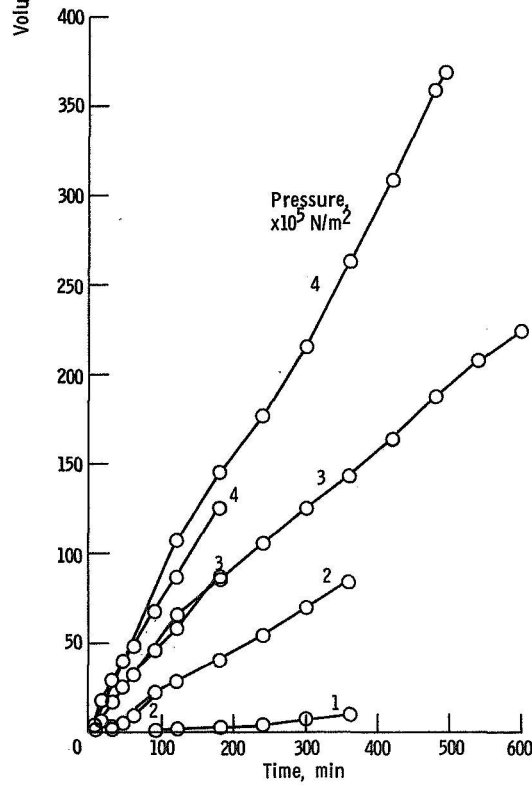


Figure 10. - Relation of cavitation damage, normalized to area basis, to ambient pressure for materials tested in 800° F (427° C) sodium

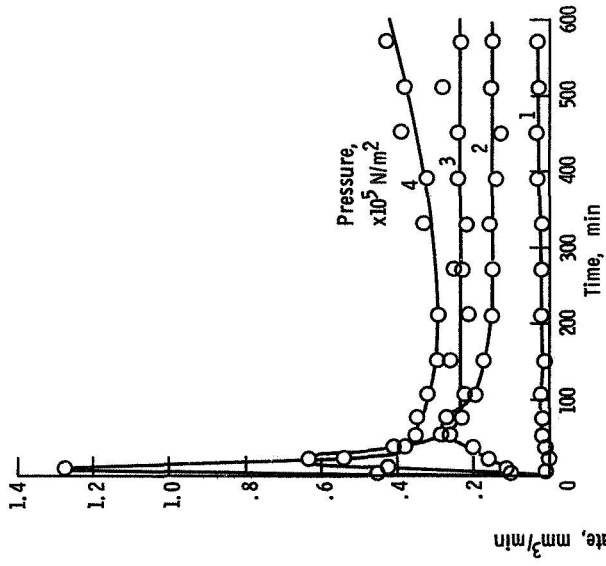


(a) Temperature, 204° C.

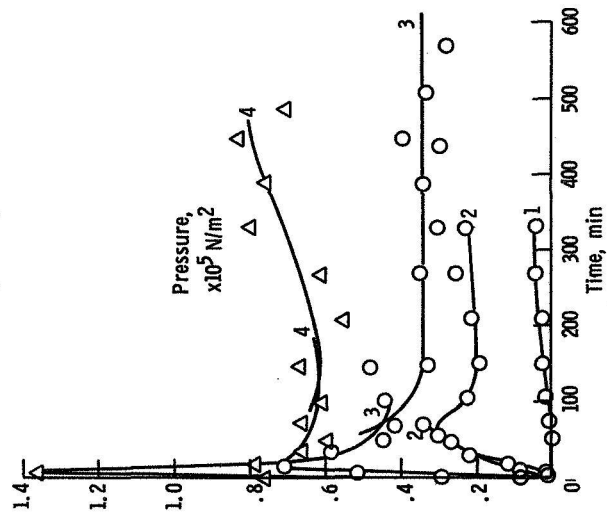


(b) Temperature, 427° C.

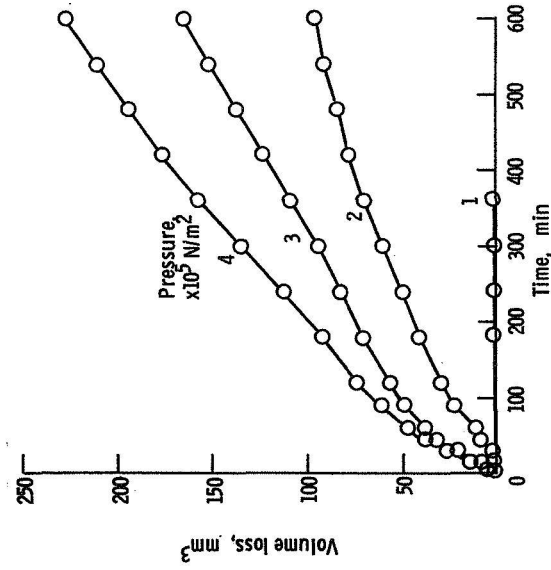
Figure 11. - Cumulative cavitation damage of L-605 tested in sodium at various temperatures and pressures.



(a) Temperature, 204° C.



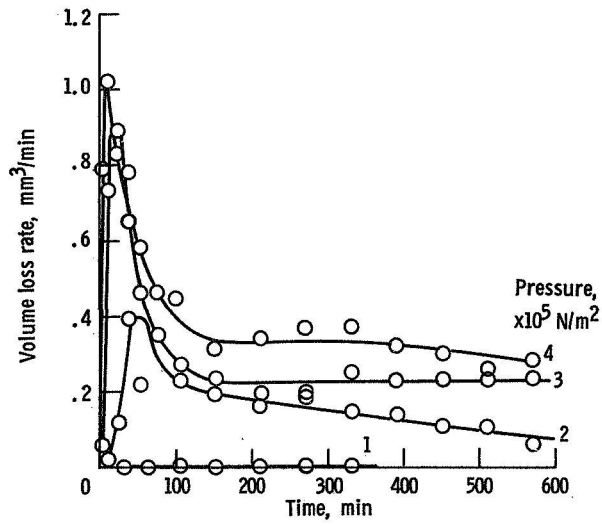
(b) Temperature, 427° C.



(c) Temperature, 649° C.

Figure 11. - Concluded.

Figure 12. - Rate of cavitation damage of L-605 specimens tested in sodium at various temperatures and pressures.



(c) Temperature, 649° C.

Figure 12. - Concluded.

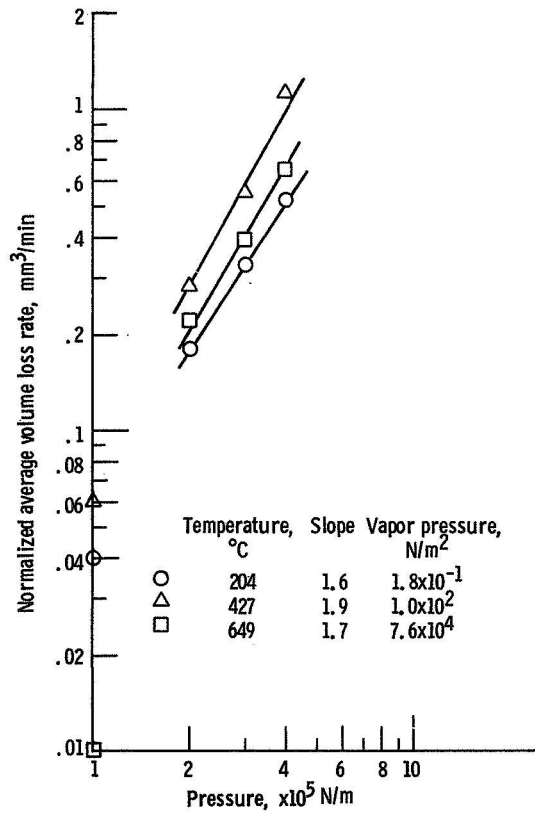


Figure 13. - Relation between normalized cavitation damage rate and ambient pressure for L-605 tested in sodium at various temperatures.

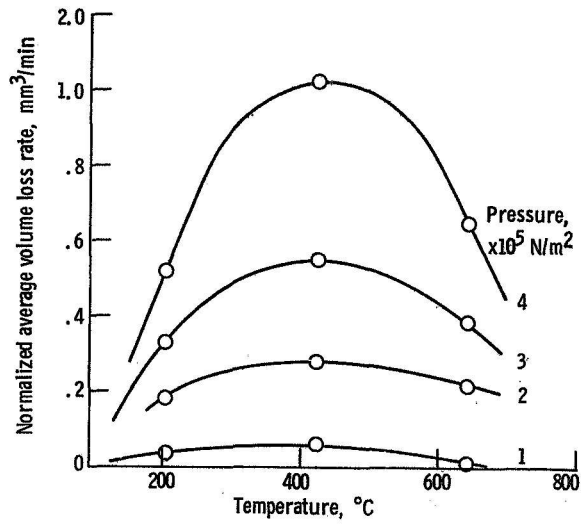


Figure 14. - Relation between normalized cavitation damage rate and temperature for L-605 tested in sodium at various pressures.

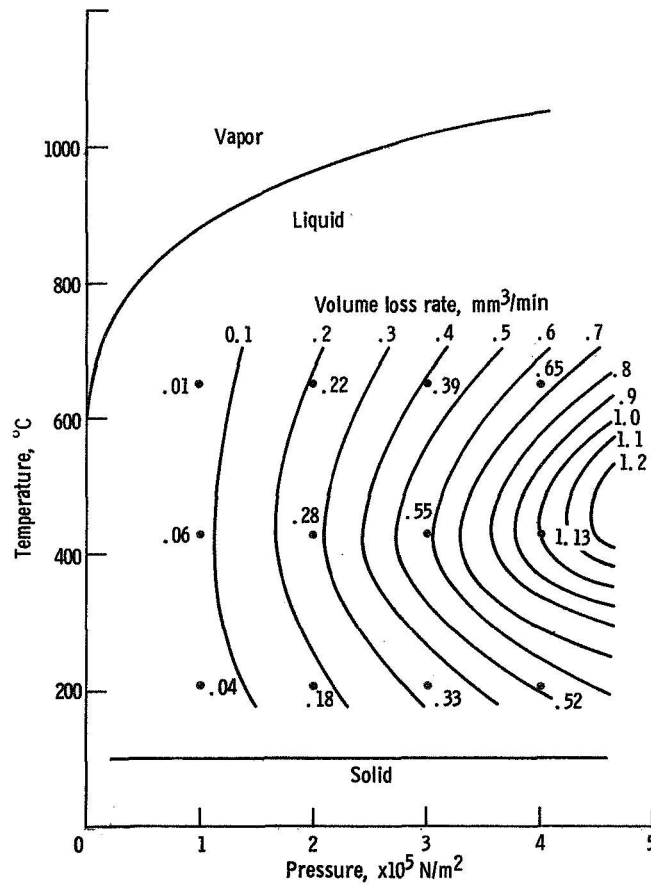


Figure 15. - Effect of temperature and pressure on normalized cavitation damage rate for L-605 tested in sodium.

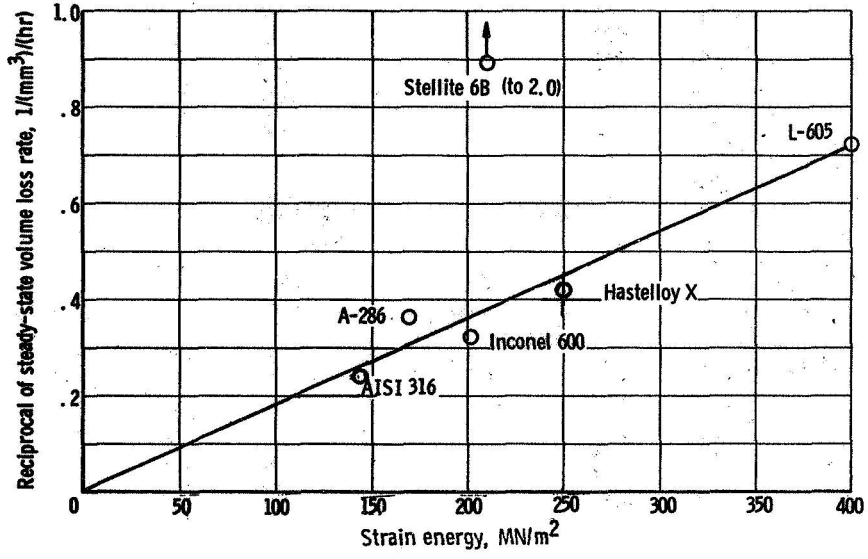
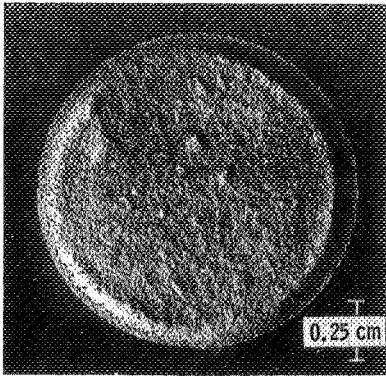
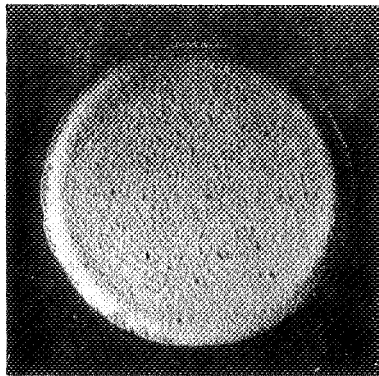


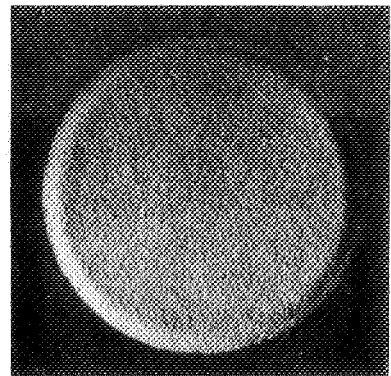
Figure 16. - Relation of cavitation damage in sodium with strain energy parameter.



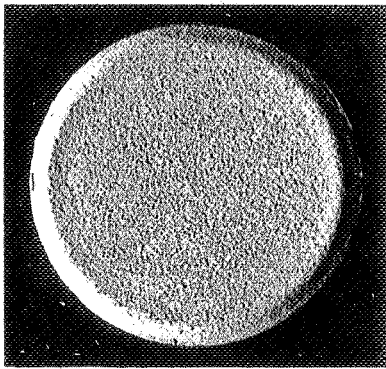
Annealed Sicromo 9M



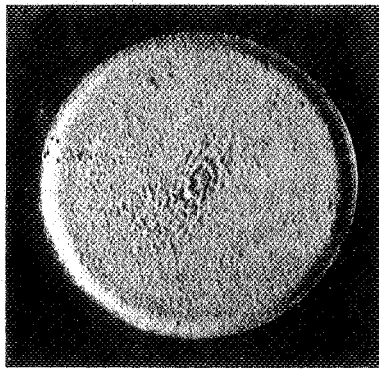
AISI 316 stainless steel



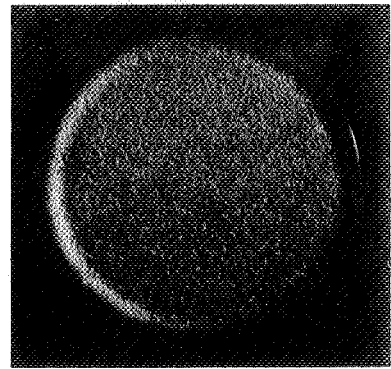
AISI 318 stainless steel



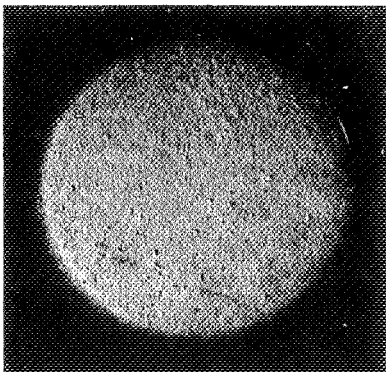
Inconel 600



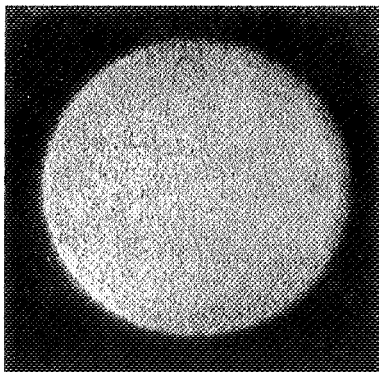
A-286



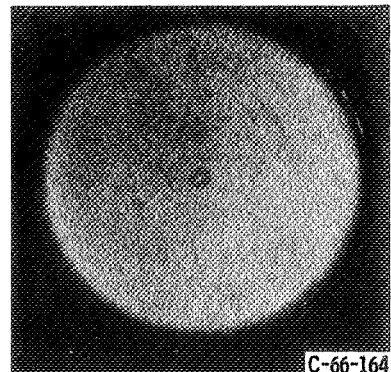
Hastelloy X



L-605

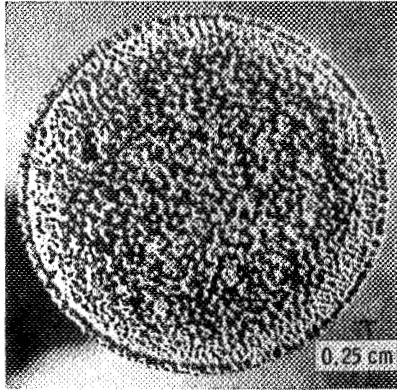


Rene 41

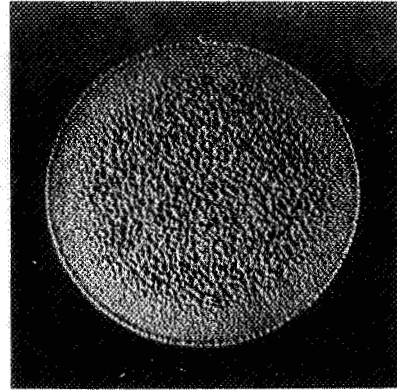


Stellite 6B

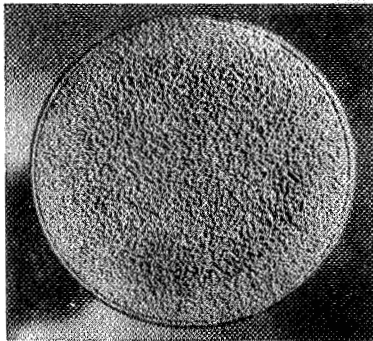
Figure 17. - Damaged surfaces of specimens after exposure to cavitation in sodium at 427° C for 4 hr.



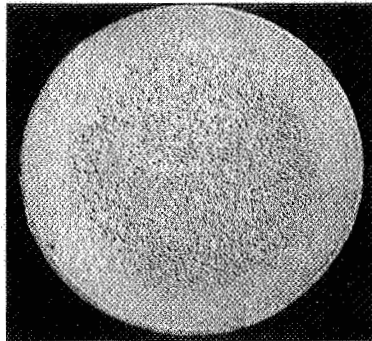
Annealed sicromo 9M (1 hr)



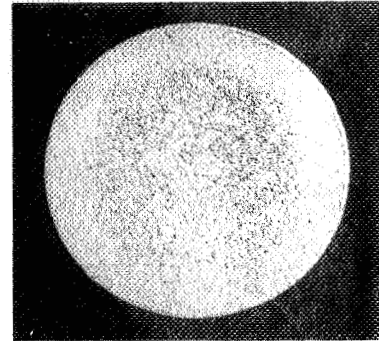
Hastelloy X (1 hr)



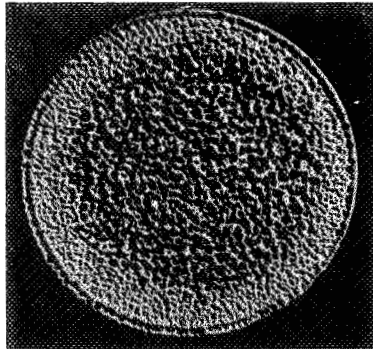
L-605 (1 hr)



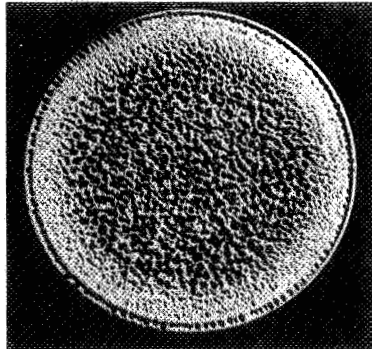
Hardened sicromo 9M (1 hr)



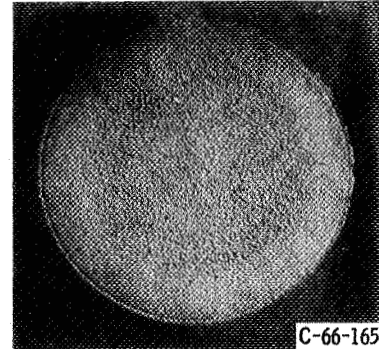
Stellite 6B (2 hr)



L-605 (4 hr)

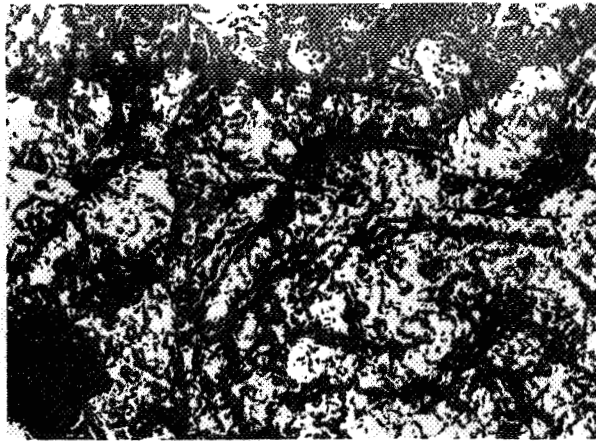


Hardened sicromo 9M (4 hr)

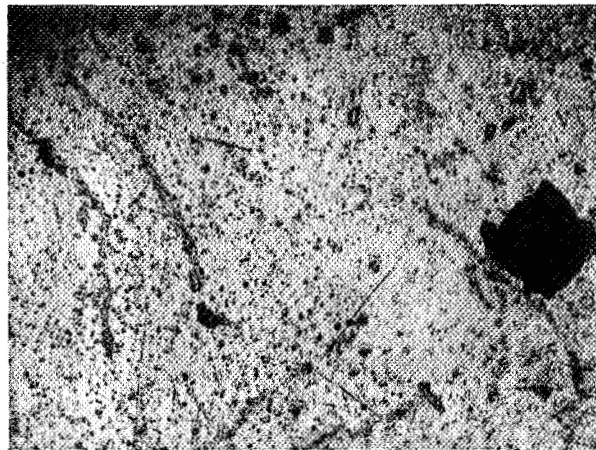


Stellite 6B (4 hr)

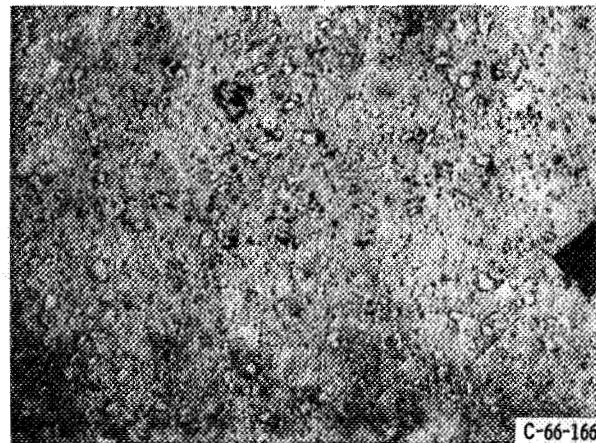
Figure 18. - Damaged surfaces of specimens after exposure to cavitation in mercury at 149° C.



(a) AISI 316 stainless steel.

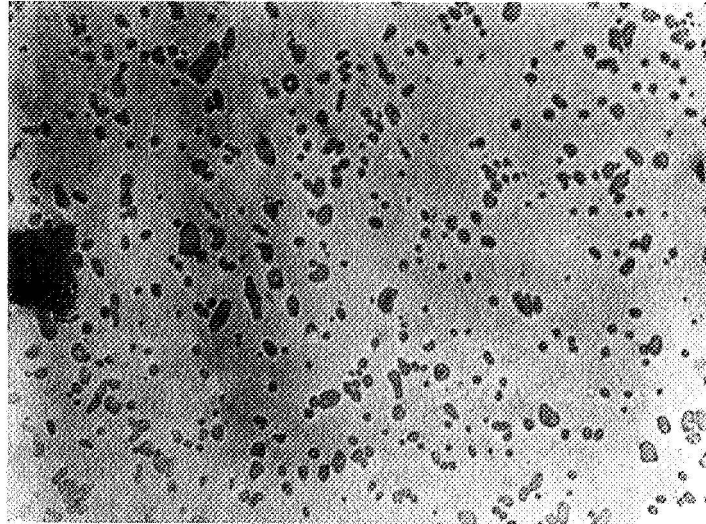


(b) L-605.

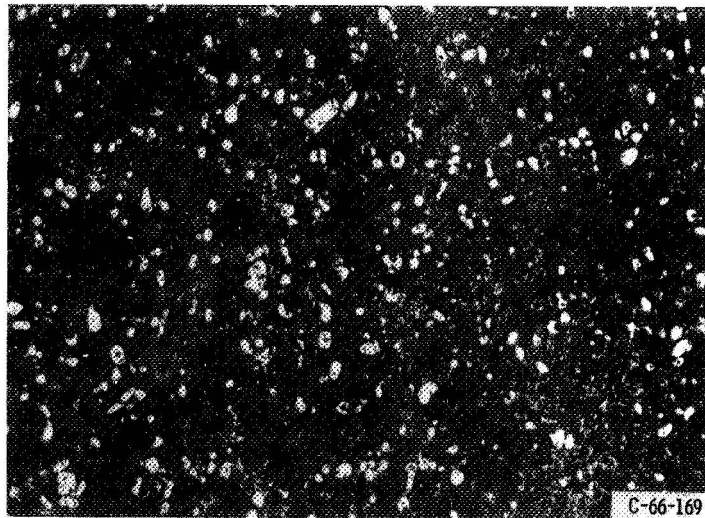


(c) Stellite 6B.

Figure 19. - Photomicrographs of damaged surfaces of specimens exposed to cavitation in sodium at 427° C for 5 min. (X250).

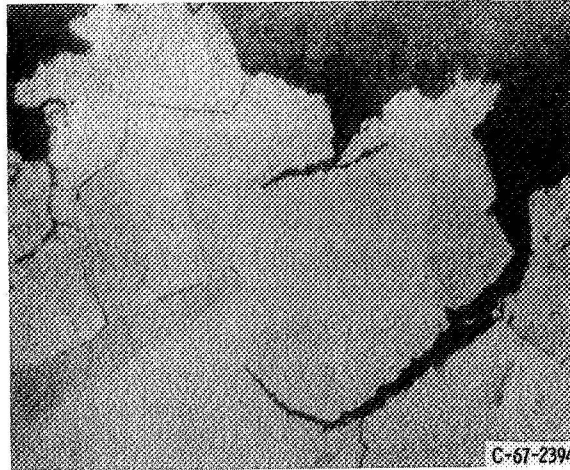


0 min

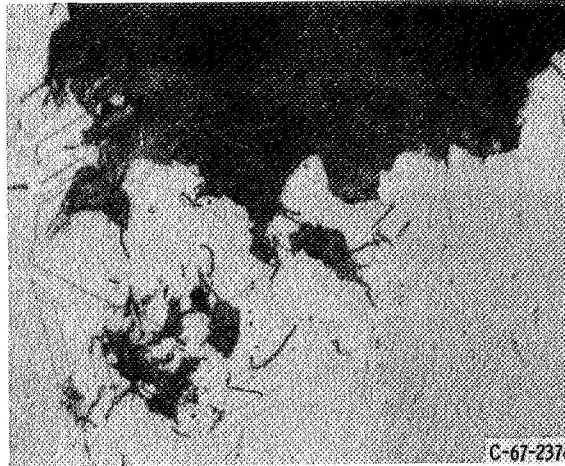


2 min

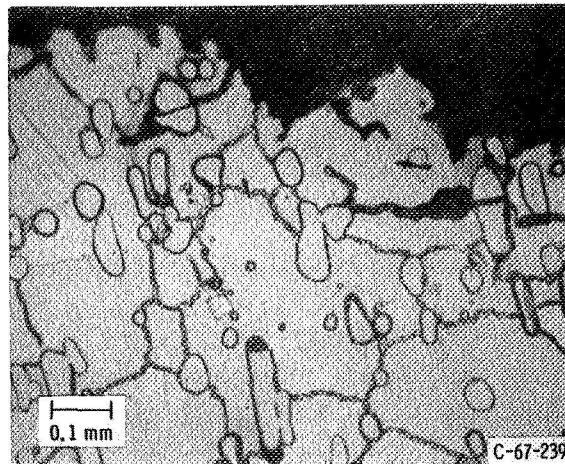
Figure 20. - Photomicrographs of damaged surface of Stellite 6B exposed to cavitation in mercury at 149° C (X250).



(a) AISI 316 stainless steel, 240-minute exposure.

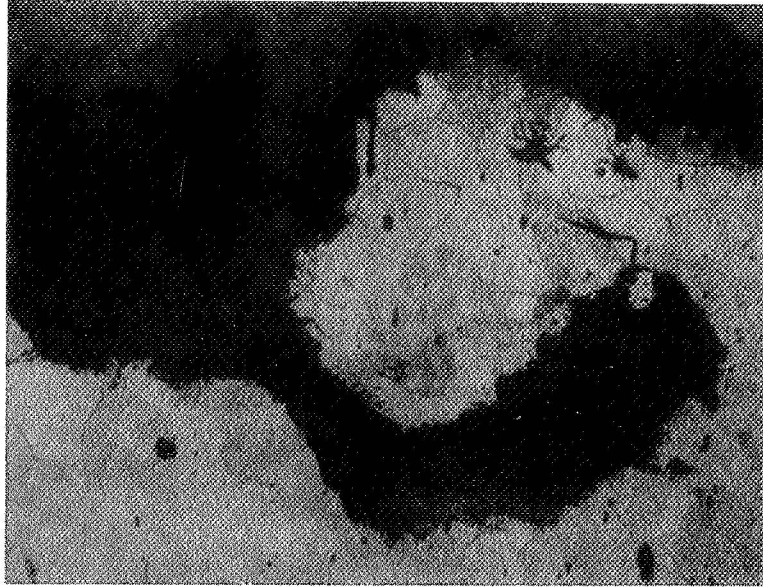


(b) L-605, 360-minute exposure.

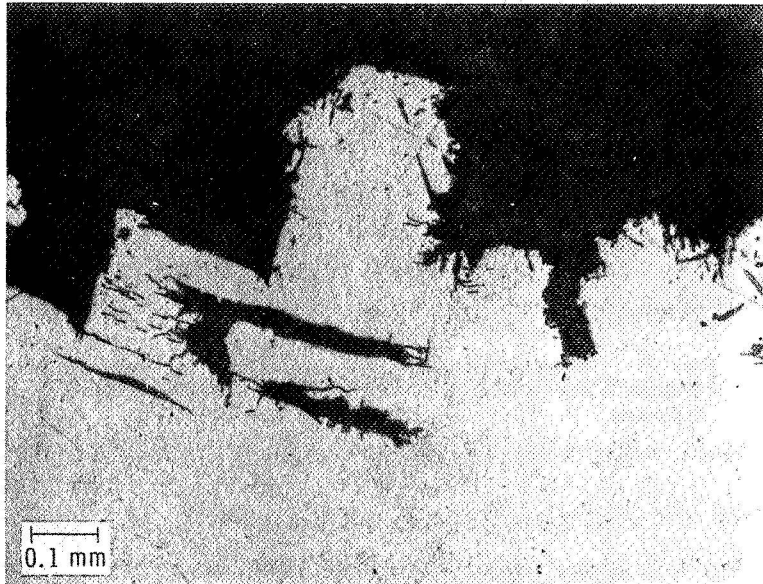


(c) Stellite 6B, 480-minute exposure.

Figure 21. - Photomicrographs of sectioned specimens after exposure to cavitation in sodium at 427° C and 4×10^5 N/m², showing damage characteristics such as undercutting and transgranular cracking.

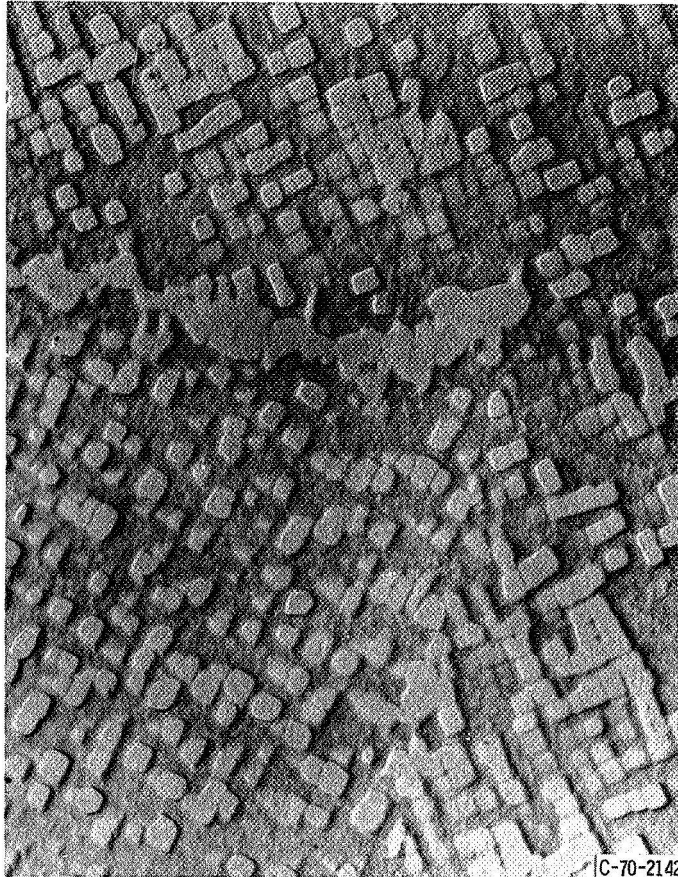


Iron; 840 min



Tantalum; 840 min

Figure 22. - Sectioned specimens of metals after exposure to cavitation in water at 24° C. (Note similarity with sodium damage characteristics - figure 19).



C-70-2142

Figure 23. - Electron microscope replica of surface of Udimet 700 subjected to cavitation in water at 24° C for 120 minutes. X17 500. (Reduced 30 percent in printing.)